Vital roles of mTOR complex 2 in Notch-driven thymocyte differentiation and leukemia

Keunwook Lee,[1] Ki Taek Nam,[2,5] Sung Hoon Cho,[1] Prathyusha Gudapati,[1] Yoonha Hwang,[3] Do-Sim Park,[1] Ross Potter,[1] Jin Chen,[3,5] Emmanuel Volanakis,[4] and Mark Boothby[1,3]

[1]Department of Pathology, Microbiology, and Immunology, [2]Department of Surgery, [3]Department of Medicine, and [4]Department of Pediatrics, Vanderbilt University School of Medicine, Nashville, TN 37232
[5]Veterans Affairs Medical Center, Tennessee Valley Healthcare System, Nashville, Nashville, TN 37212

Notch plays critical roles in both cell fate decisions and tumorigenesis. Notch receptor engagement initiates signaling cascades that include a phosphatidylinositol 3-kinase/target of rapamycin (TOR) pathway. Mammalian TOR (mTOR) participates in two distinct biochemical complexes, mTORC1 and mTORC2, and the relationship between mTORC2 and physiological outcomes dependent on Notch signaling is unknown. In this study, we report contributions of mTORC2 to thymic T-cell acute lymphoblastic leukemia (T-ALL) driven by Notch. Conditional deletion of Rictor, an essential component of mTORC2, impaired Notch-driven proliferation and differentiation of pre-T cells. Furthermore, NF-κB activity depended on the integrity of mTORC2 in thymocytes. Active Akt restored NF-κB activation, a normal rate of proliferation, and differentiation of Rictor-deficient pre-T cells. Strikingly, mTORC2 depletion lowered CCR7 expression in thymocytes and leukemic cells, accompanied by decreased tissue invasion and delayed mortality in T-ALL driven by Notch. Collectively, these findings reveal roles for mTORC2 in promoting thymic T cell development and T-ALL and indicate that mTORC2 is crucial for Notch signaling to regulate Akt and NF-κB.

CORRESPONDENCE
Mark Boothby:
mark.boothby@vanderbilt.edu

Abbreviations used: cKO, conditional KO; DN, double negative; DP, double positive; EMSA, electrophoretic mobility shift assay; FSC, forward scatter; HM, hydrophobic motif; mRNA, messenger RNA; PH, pleckstrin homology; PI3K, phosphatidylinositol 3-kinase; PKC, protein kinase C; RNAi, RNA interference; T-ALL, T-cell acute lymphoblastic leukemia; TOR, target of rapamycin.

Developmental progression in thymocytes is regulated by signal transduction nodes that integrate inputs from cytokine and antigen receptors with those for ligands on stromal cells. Progression through stages as $CD4^-CD8^-$ double-negative (DN) precursors until the completion of TCR rearrangement and differentiation into $CD4^+CD8^+$ double-positive (DP) thymocytes involves signaling initiated by pre-TCR, IL-7R, and Notch (Hayday and Pennington, 2007). The Notch family consists of four conserved transmembrane receptors normally activated by ligands of the Delta/Jagged family expressed on neighboring cells; this activation by ligand releases an intracellular domain of Notch (ICN) from the plasma membrane to the nucleus to regulate expression of target genes such as *Hes1* and the proto-oncogene *Myc* (Maillard et al., 2005). Notch1 regulates T lineage progression at specific steps that include proliferative expansion of DN thymocytes and their differentiation into DP cells (Radtke et al., 1999; Tanigaki et al., 2004; Maillard et al., 2005). How specific signal transduction pathways mediate these effects is not clear. One insight from an in vitro study has been that Notch ligation promotes glycolytic metabolism, and the Notch signal could be made superfluous by overexpression of Myr-Akt (Ciofani and Zúñiga-Pflücker, 2005). This constitutively active mutant of the serine-threonine kinase Akt sufficed to support enhanced cellular metabolism, proliferation, and generation of DP cells even in cultures on OP9 cells lacking the Notch ligand DL1 (Delta-like 1; Ciofani and Zúñiga-Pflücker, 2005). This finding suggested that pathways downstream from the lipid kinase phosphatidylinositol 3-kinase (PI3K) play key roles in Notch-induced thymocyte progression in vivo and that Notch promotes this progression at the β-selection checkpoint by regulating cellular metabolism.

The Rockefeller University Press $30.00
J. Exp. Med. Vol. 209 No. 4 713-728
www.jem.org/cgi/doi/10.1084/jem.20111470

Physiological activation of Akt involves the generation of phosphatidylinositol 3, 4, 5-triphosphate (PIP3) by PI3K, recruitment of Akt to membranes via its pleckstrin homology (PH) domain, and obligate T-loop (T308) phosphorylation by PDK1 (PI3K-dependent kinase 1; Vanhaesebroeck and Alessi, 2000). Inactivation of PDK1 early in T lineage ontogeny blocked thymic differentiation at a DN stage, and PDK1-null pre-T cells did not respond to Notch-induced trophic, proliferative, or differentiating signals (Hinton et al., 2004; Kelly et al., 2007). Similar phenotypes were observed when the genes encoding multiple isoforms of Akt were inactivated in T lineage cells (Juntilla et al., 2007; Mao et al., 2007). These results indicate that expression of Akt and the capacity to execute its T-loop phosphorylation by PDK1 are vital at the DN to DP transition. The ability of Notch to drive PI3K/Akt-related pathways is notable because in addition to its roles in thymic development, Notch is important in oncologic pathophysiology (Weng et al., 2004; O'Neil et al., 2006). Gain of function mutations of Notch are implicated in a variety of cancers, including over half of human T-cell acute lymphoblastic leukemia (T-ALL; Weng et al., 2004). Consistent with an important role of lipid signaling via PIP3, a major tumor suppressor impacts the pathway by dephosphorylating PIP3 to regenerate PIP2 (Cully et al., 2006), and unbiased screens identified Akt mutation and loss of the PIP3-phosphatase PTEN (phosphatase and tensin homologue) as major contributors in malignancy (Li et al., 1997; Eng, 2003; Carpten et al., 2007; Maser et al., 2007; Gutierrez et al., 2009). Use of a transdominant inhibitor of NF-κB activation indicated that this transcriptional pathway is a key relay activated by Notch in T-ALL (Vilimas et al., 2007), but little is known about crucial intermediaries in the process.

Akt can also be phosphorylated at a C-terminal hydrophobic motif (HM; "S473") by activities referred to as PDK2 (Chan and Tsichlis, 2001). In addition to the original rapamycin-sensitive complex containing mammalian target of rapamycin (mTOR), complex 1 (mTORC1), this kinase participates in a second complex, mTORC2 (Sarbassov et al., 2004), which, unlike mTORC1, is resistant to acute rapamycin inhibition (Sarbassov et al., 2006). MTORC2, whose integrity requires rictor, mSIN1, and mLST8 subunits in addition to mTOR, appeared to be the sole PDK2 responsible for Akt HM phosphorylation in several cancer cells and mouse embryonic fibroblasts (Sarbassov et al., 2005; Guertin et al., 2006; Shiota et al., 2006). Deficiency in any subunit impacted mTORC2 activity as a PDK2 toward substrates such as Akt, SGK1, and protein kinase C (PKC) isoforms (Guertin et al., 2006; Jacinto et al., 2006; García-Martínez and Alessi, 2008). Whereas PH domain binding to PIP3 and T308 phosphorylation of Akt by PDK1 are essential for turning on the kinase (Sarbassov et al., 2005; Laplante and Sabatini, 2009), Akt HM phosphorylation at most modulates Akt activity. Depletion of rictor impaired Akt S473 phosphorylation in resting and activated mature T cells (Lee et al., 2010; Delgoffe et al., 2011). However, residual HM phosphorylation of Akt consistent with the capacity of other enzymes to phosphorylate the Akt S473 was observed in studies in which rictor was deleted after differentiation of thymocytes to a positively selecting DP stage (Lee et al., 2010) or when the *CD4*-Cre transgene, which acts in late DN cells, was used (Delgoffe et al., 2011). Thus, it was possible that the capacity of alternative kinases such as DNA-PKs (Feng et al., 2004), PKC-β (Kawakami et al., 2004), or IκB kinase ε and TANK (TRAF-associated NF-κB activator)-binding kinase 1 (Xie et al., 2011) to execute direct Akt HM phosphorylation might provide sufficient activity in thymocytes. Nonetheless, the requirement for Akt in thymic ontogeny before β-selection and a connection of Notch to Akt do not establish what quantitative level of Akt activity might be needed for specific aspects of the process. Accordingly, it is not clear whether mTORC2 or HM phosphorylation of Akt impacts thymocyte development or pathological consequences of sustained, high-level Notch signaling.

Herein, we used the in vitro model system that compares stromal cells (OP9) that express the Notch ligand DL1 (OP9-DL1) to isogenic OP9 controls (Ciofani and Zúñiga-Pflücker, 2005) to identify outcomes that are changed by a Notch signal. Signaling, size, glycolysis, proliferation, and differentiation of WT and mTORC2-depleted thymocytes were compared after culture on OP9 ± DL1. Because lack of mTORC2 impaired Notch-induced proliferation and differentiation of DN into DP thymocytes, we analyzed the impact of the loss of function mutation on thymic development and disease progression of T-ALL driven by Notch. Overall, our results indicate that mTORC2 relays a Notch signal to NF-κB to regulate the *Ccr7* gene, contributing to thymic T cell development and T-ALL.

RESULTS

A loss of function model for PDK2 activity in thymocytes

To investigate the role of mTORC2 in Notch effects on thymocytes, an essential subunit was conditionally depleted by breeding *Rictor*$^{fl/fl}$ mice with transgenic mice expressing Cre controlled by the *Lck* proximal promoter (*Lck-Cre*$^{+}$ *Rictor*$^{fl/fl}$; abbreviated hereafter as conditional KO [cKO]). Cells from these mice were then compared with WT controls that included *Lck-Cre*$^{+}$ *Rictor*$^{WT/WT}$ as well as *Rictor*^{fl} mice lacking a Cre transgene (no difference of results was observed between these two classes of WT control). Excision of the conditional allele by Cre was observed early in T ontogeny, starting at the DN2 stage, and resulted in *Rictor* deletion in cKO thymocytes and peripheral T cells but not in the non-T populations (Fig. 1, A and B). Moreover, Rictor protein was depleted in the cKO thymocytes, whereas mTOR did not change (Fig. 1 C). TORC2 and other serine-threonine kinases can phosphorylate Akt at its C-terminal HM (S473; Feng et al., 2004; Kawakami et al., 2004; Xie et al., 2011). Loss of Rictor eliminated most PDK2 activity toward Akt S473 both in resting and costimulated thymocytes but did not substantially reduce Akt phosphorylation at T308, the PDK1 target site (Fig. 1 D). Also, Akt enzymatic activity was markedly decreased in the rictor-depleted thymocytes (Fig. 1 E). Consistent with these effects, phosphorylation of the Akt substrate FoxO1/3a was impaired

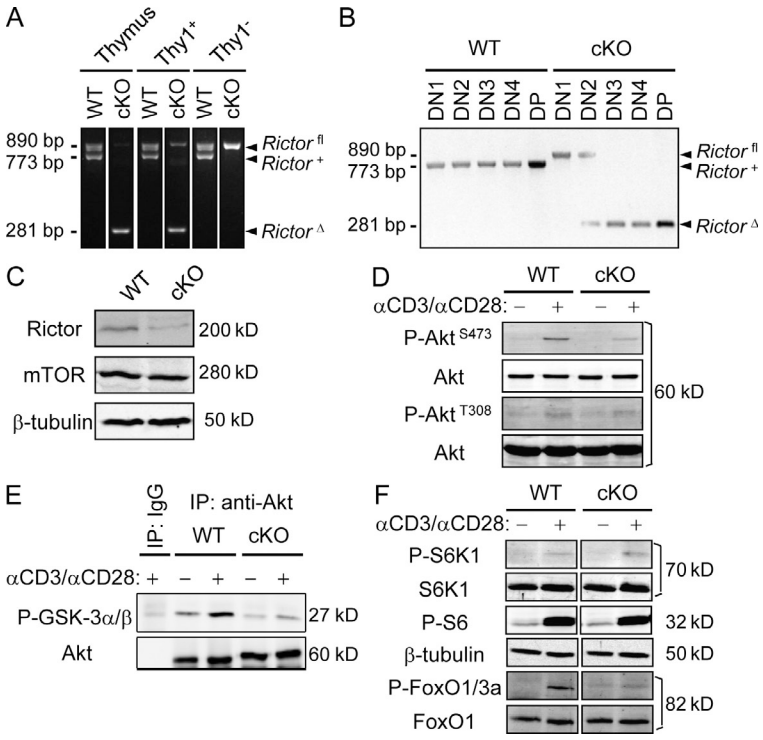

Figure 1. Akt S473 phosphorylation and Akt activity in thymocytes depend on Rictor. (A and B) Cre-driven *Rictor* deletion. (A) DNA was prepared from thymocytes and peripheral lymphoid cells fractionated using Thy1. Shown is a PCR detecting *Rictor* of WT (+), conditional (fl), and deleted (Δ) alleles from the indicated mice (WT, *Lck*-Cre$^-$ *Rictor*$^{fl/+}$; cKO, *Lck*-Cre$^+$ *Rictor*$^{fl/fl}$; representative of three replicates). (B) Shown is a result (one of two) for PCR detecting *Rictor* alleles, as in A, using DNA from DN thymocyte subsets flow sorted by CD25 and CD44 expression on CD4$^-$CD8$^-$ cells. (C) Immunoblot analysis of rictor and mTOR in thymocytes, normalized to β-tubulin signal (one of three independent experiments). (D) *Rictor*-null thymocytes were stimulated with 2.5 µg/ml anti-CD3 and 2.5 µg/ml anti-CD28 and analyzed by immunoblots with the indicated antibody (one representative of four independent experiments, except $n = 2$ for P-Akt(T308)). (E) Using GSK-3α/β as a substrate, enzymatic activity was assayed in the anti-Akt complexes immunoprecipitated from thymocyte lysates. Shown is an anti-P-GSK-3 immunoblot result (one representative of two independent experiments). IP, immunoprecipitation. (F) P-FoxO expression in *Rictor* cKO cells, showing the (P-)FoxO1 bands after immunoblot analyses as in D.

(Fig. 1 F). Increased Akt activity can potentially enhance mTORC1 (Kelly et al., 2007; Dan et al., 2008; Laplante and Sabatini, 2009) but in Rictor-deficient thymocytes exhibited no decrease in phosphorylation of S6K1 downstream from mTORC1 or its target S6. PDK2 activity is robust in the absence of mTOR in some settings (Bentzinger et al., 2008; Xie et al., 2011), and our data suggest that there may be a secondary PDK2 in thymocytes. Nonetheless, mTORC2 served as the main kinase for Akt S473 in thymocytes, and this HM phosphorylation enhanced Akt activity and FoxO phosphorylation.

Notch-driven proliferation and differentiation of thymocytes depend on *Rictor*

To analyze roles of mTORC2 and HM phosphorylation of Akt in Notch-driven thymocyte progression, we used an in vitro system with OP9 stromal cells expressing the Notch ligand DL1 (Fig. 2 A; Ciofani and Zúñiga-Pflücker, 2005). As expected, WT DN cells exhibited rapid proliferation (~30-fold increase) and differentiation into DP thymocytes (30–40% of cells) when cultured on the OP9-DL1 (Fig. 2, B and C). In contrast, *Rictor*-null DN cells proliferated and differentiated far less efficiently on OP9-DL1 (Fig. 2, B and C). To test whether Notch ligand was less able to restrict the DN population to T lineage fates in the *Rictor*-null thymocytes, Thy1 was measured on nonstromal cells in OP9-DL1 cultures, but 98–99% of cells were Thy1$^+$ (Fig. 2, D and E). The few DN1 and DN2 cells at the outset of a culture need ongoing Notch signals to adopt or maintain a T lineage fate (Schmitt et al., 2004). A substantial majority of *Rictor* cKO cells at the end of cultures on OP9 without Notch ligand were Thy1$^+$, and there was only a modest difference between WT- and cKO-derived cells as to frequencies of NK1.1$^+$ and Gr1$^+$ cells (Fig. 2, D and E). Furthermore, purified DN3 cells yielded >98% Thy1$^+$ products from *Rictor* cKO as well as WT thymi after co-culture with OP9 (not depicted). As in the work connecting mTOR to Notch, these cultures were supplemented with IL-7 (Ciofani and Zúñiga-Pflücker, 2005). In the absence of IL-7, DN thymocytes barely multiplied in response to DL1, but in any case, Notch-induced differentiation and proliferation of the cKO DN cells were less than controls (Fig. 2 F and not depicted). These results demonstrate a requirement for mTORC2 in the proliferation and differentiation of pre-T cells in a Notch-dependent setting. Furthermore, although myriad receptors, including the pre-TCR and IL-7R, signal in this system, the findings suggest that the need for Rictor represents PI3K and mTORC2 downstream from Notch in attainment of full proliferation and DN to DP progression.

Notch promoted pre-T cell metabolism and thereby survival and proliferation; the rapamycin sensitivity of these processes implicated mTOR but cannot definitively distinguish whether the signals are relayed by mTORC1, mTORC2, or both (Ciofani and Zúñiga-Pflücker, 2005; Sarbassov et al., 2006; Kelly et al., 2007; Lee et al., 2010). Consistent with prior analyses, we observed increases in the size (forward scatter [FSC] of light) and glycolytic rate of WT DN thymocytes cultured on OP9-DL1 as compared with OP9 without Notch ligand (Fig. 2, G and H). Despite their reduced proliferation, cKO DN cells were comparable with WT controls in measurements of size and glycolytic rate (Fig. 2, G and H). Notch-driven PI3K suppresses caspase-3 cleavage in pre-T cells, and results of rapamycin inhibition along with loss of function for PDK1 suggest that PDK1 and mTOR are important for Notch inhibition of apoptosis (Ciofani and Zúñiga-Pflücker, 2005;

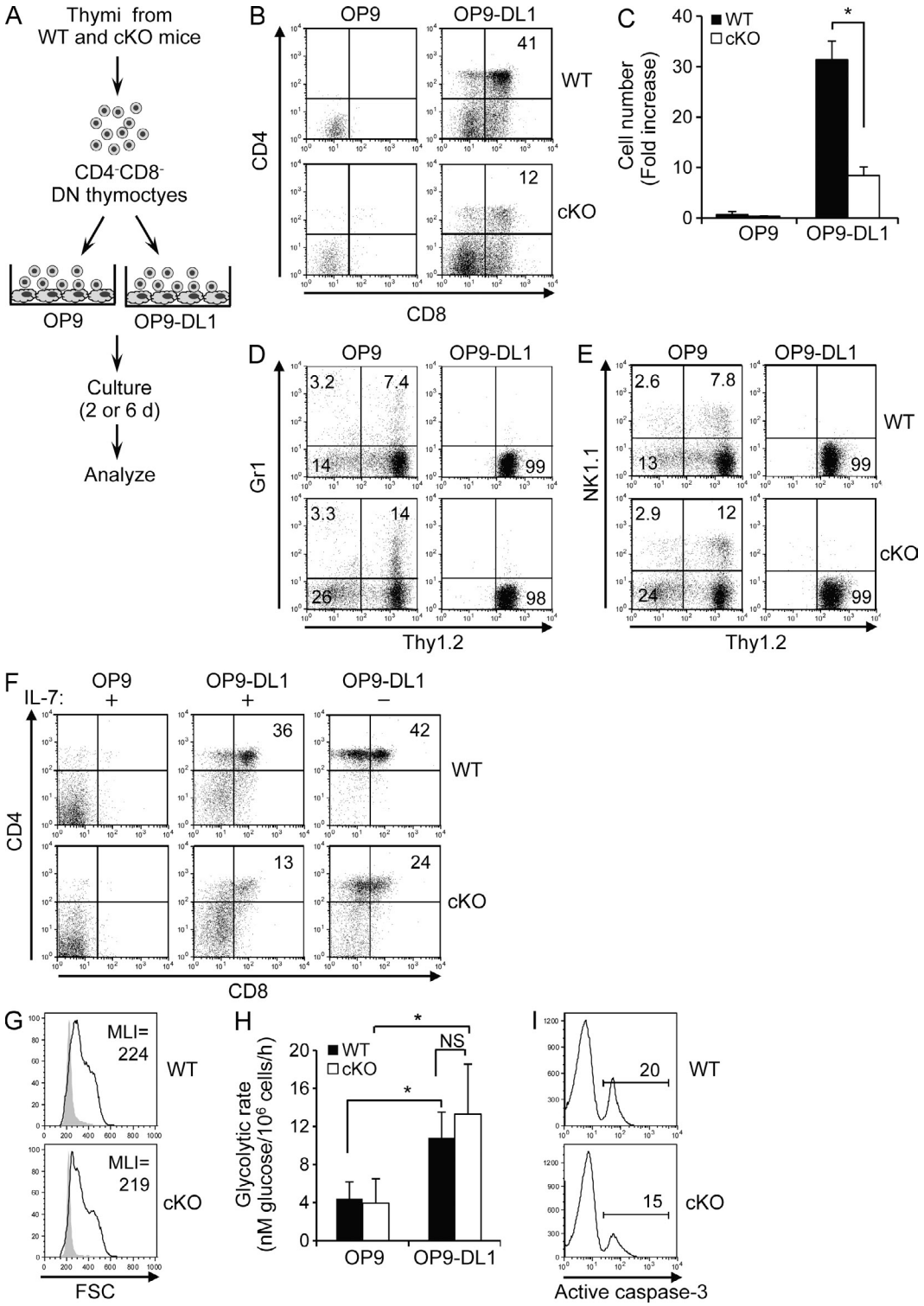

Figure 2. Notch-driven proliferation and differentiation of DN thymocytes but not their glycolytic rate require Rictor. (A) The assay system. Purified $CD4^{-}CD8^{-}$ thymocytes were cultured on isogenic stromal cells bearing Notch ligand (OP9-DL1) or control OP9 cells in the presence or absence of IL-7. (B) Effect of Rictor on DN thymocyte differentiation. Shown is a CD4 and CD8 flow analysis of DN cells cultured with OP9-DL1 or control OP9 monolayers for 6 d; the inset numbers indicate the percentage of $CD4^{+}CD8^{+}$ (DP) cells (one representative result of four independent replicates). (C) DN thymocyte proliferation after *Rictor* deletion. Shown are the means (±SEM; $n = 4$ experiments) for thymocyte expansion in the culture (fold increase = cells recovered/input DN cells). *, $P < 0.05$. (D and E) DN thymocytes cultured as in B were analyzed for surface markers of T-, myeloid-, and NK/NKT-lineage progeny (D–F: one result of four samples, from two independent experiments, each performed in duplicate). (F) Purified DN thymocytes were cultured for

Kelly et al., 2007). However, Rictor-deficient thymocytes did not exhibit increased activated caspase-3 compared with WT controls (Fig. 2 I). Thus, the impaired multiplication and DN to DP transition of PDK2-deficient thymocytes appear to be uncoupled from suppression of atrophy (cell size and glycolysis) and caspase activation.

Akt mediates mTORC2 signaling downstream from Notch

To test whether the DN thymocyte fraction exhibited any abnormality of Akt activity or FoxO phosphorylation in a setting more closely modeled on the Notch-driven differentiation system, $CD4^{-}CD8^{-}$ cells were cultured on OP9-DL1 stromal cells for 2 d. Although cell numbers were limiting even with Notch ligand, purified DN thymocytes cultured on Notch ligand–bearing stromal cells exhibited substantially reduced phosphorylation of the Akt HM and of FoxO1/3a in Rictor-deficient samples (Fig. 3 A). Of note, the Notch ligand on the OP9-DL1 stromal cells enforced essentially complete maintenance of T lineage commitment, and little differentiation to DP status was evident. Moreover, the amounts of cleaved intracellular Notch and S6 phosphorylation in the WT and cKO thymocytes of these cultures were similar (Fig. 3 A). We conclude that stimulus-induced Akt activity in pre-T cells depends on their mTORC2.

We next transduced DN cells to test whether activated Akt could restore normal proliferation or differentiation of Rictor-depleted thymocytes in the OP9-DL1 co-culture system. In line with earlier work (Ciofani and Zúñiga-Pflücker, 2005), we tested Myr-Akt, which bypasses the physiological role of PH domain–mediated binding to PIP3 (Fig. 3 B). Transduction with Myr-Akt enhanced differentiation for WT DN cells and drove cKO DN cells to develop into DP cells as efficiently as their WT counterparts (Fig. 3 B). As expected (Ciofani and Zúñiga-Pflücker, 2005), Myr-Akt drove WT DN cells to proliferate and develop into DP cells even in the absence of Notch ligand and drove cKO thymocytes cultured on OP9-DL1 to yield as many DP cells as their WT counterparts (not depicted). We next used two isogenic variants of constitutively active Akt that retains its PH domain, one of which encodes phosphomimetic aspartates at both the T loop and HM phosphorylation sites (Akt(DD): T308D S473D). Transduction of DN thymocytes with Akt(DD) only weakly induced proliferation and differentiation into DP cells in the absence of Notch ligand but enhanced these processes in WT cells cultured on OP9-DL1 (Fig. 3, C–E). Importantly, Akt(DD) substantially increased both proliferation and the efficiency of differentiation of Notch-stimulated Rictor-deficient DN thymocytes, attaining almost WT values (Fig. 3, C–E). To test whether active Akt that cannot be phosphorylated at the HM could fully replace the signals lacking in the absence of mTORC2, Akt(DA) (T308D S473A) was also transduced into the cKO DN cells. Intriguingly, this form of Akt enhanced proliferation to an extent similar to Akt(DD) but provided little rescue of differentiation (Fig. 3, C–E). These data indicate that mTORC2 relays Notch signaling in part by phosphorylation of Akt S473 in thymocytes and suggest that there are distinct activity–response curves for differentiation and proliferation of pre-T cells.

mTORC2 regulates nuclear localization of NF-κB in thymocytes

Nuclear translocation of the transcription factor NF-κB is triggered by both the pre-TCR and Notch during thymic development (Voll et al., 2000; Vacca et al., 2006), so we analyzed whether mTORC2 impacts thymocyte NF-κB. Nuclear NF-κB DNA-binding activities were decreased in the cKO thymocytes compared with controls (Fig. 4 A). Of note, ample nuclear NF-κB was detected after 2-d culture in DL1-stimulated WT DN thymocytes but not in the cKO cells or those cultured on OP9 alone in the co-culture system with IL-7 present and all factors the same except the additional Notch ligand (Fig. 4 B). To explore the impact of this defect, we measured expression of several NF-κB target genes. Expression of *Bcl2a1* and *Nfkb2* was decreased in both DN thymocytes of cKO mice (Fig. 4 C) and Rictor-deficient DN cells cultured on OP9-DL1 (Fig. 4 D). Antibody blocking experiments demonstrated that the DNA–protein complexes contained predominantly p50:RelA heterodimers (Fig. 4 E). Thus, mTORC2 regulates NF-κB activity and target gene expression in resting thymocytes and those stimulated via Notch.

In PTEN-deficient cells, Akt can use a Raptor-dependent mechanism to activate NF-κB signaling by phosphorylating IKK-α, but the generality of this connection or the ability of Akt to increase NF-κB in the nucleus is not entirely clear (Ozes et al., 1999; Romashkova and Makarov, 1999; Jones et al., 2005; Dan et al., 2008). To test whether the NF-κB in Rictor-depleted thymocyte nuclei could be restored by activated Akt, DN cells were transduced with Akt and cultured on OP9-DL1. Akt(DD) induced NF-κB nuclear localization in the cKO DN cells of a magnitude comparable with that of WT cells (Fig. 4 F). In contrast, Akt(DA) failed to restore the NF-κB nuclear induction in the cKO DN thymocytes. We infer that mTORC2 is a relay vital for Notch induction of NF-κB in thymocytes, acting at least in part through Akt HM phosphorylation as an intermediary.

6 d on OP9-DL1 or OP9 cells in the presence or absence of IL-7 and analyzed by flow cytometry. Shown are the CD4 versus CD8 profiles of cells in the viable lymphoid gate (one result of two experiments). (G) WT and cKO DN thymocytes were cultured for 2 d on OP9-DL1, and histograms of their FSC were compared. Shaded histograms, cultured on OP9; line histograms, cultured on OP9-DL1, with mean light intensity (MLI) values shown (one result of four experiments). (H) Mean (±SEM; $n = 2$ independent experiments) glycolytic rates in purified DN cells cultured for 2 d on OP9 or OP9-DL1 cells. *, $P < 0.05$. (I) Activated caspase-3 in DN thymocytes co-cultured with OP9-DL1 (6 d). Shown are the flow histograms for cleaved caspase-3 in the viable lymphoid gate from a representative experiment (two independent replicates); inset numbers represent the percentage of positive events.

To explore further the functional implications of this dependency of Notch-induced NF-κB on mTORC2, we quantitated expression of several genes regulated by Notch, FoxO, or NF-κB. *Hes1*, a direct target of the transcriptional complex of cleaved, intracellular Notch with CSL-MAML, was marginally decreased in purified DN thymocytes analyzed directly ex vivo (Fig. 4 G). Similarly, messenger RNA (mRNA) encoding the pre-TCR α chain (*Ptcra*, encoding pTα) decreased only marginally (Fig. 4 G), and the expression of pTα and Notch proteins was unaffected by lack of Rictor (not depicted). In contrast, the FoxO targets *Il7r* and *Sell* were present at lower levels, whereas *S1p1* was not. Notably, expression of the NF-κB–regulated gene *Ccr7* was substantially decreased both in DN thymocytes from cKO mice (Fig. 4 G) and in Rictor-deficient DN cells cultured on OP9-DL1 (Fig. 4 H). Furthermore, chemotaxis of cKO cells toward CCL19, a CCR7 ligand, was decreased compared with WT controls (Fig. 4 I). These results indicate that mTORC2 is important for Notch-initiated, NF-κB–dependent gene expression but also suggest an interplay with FoxO transcription factors.

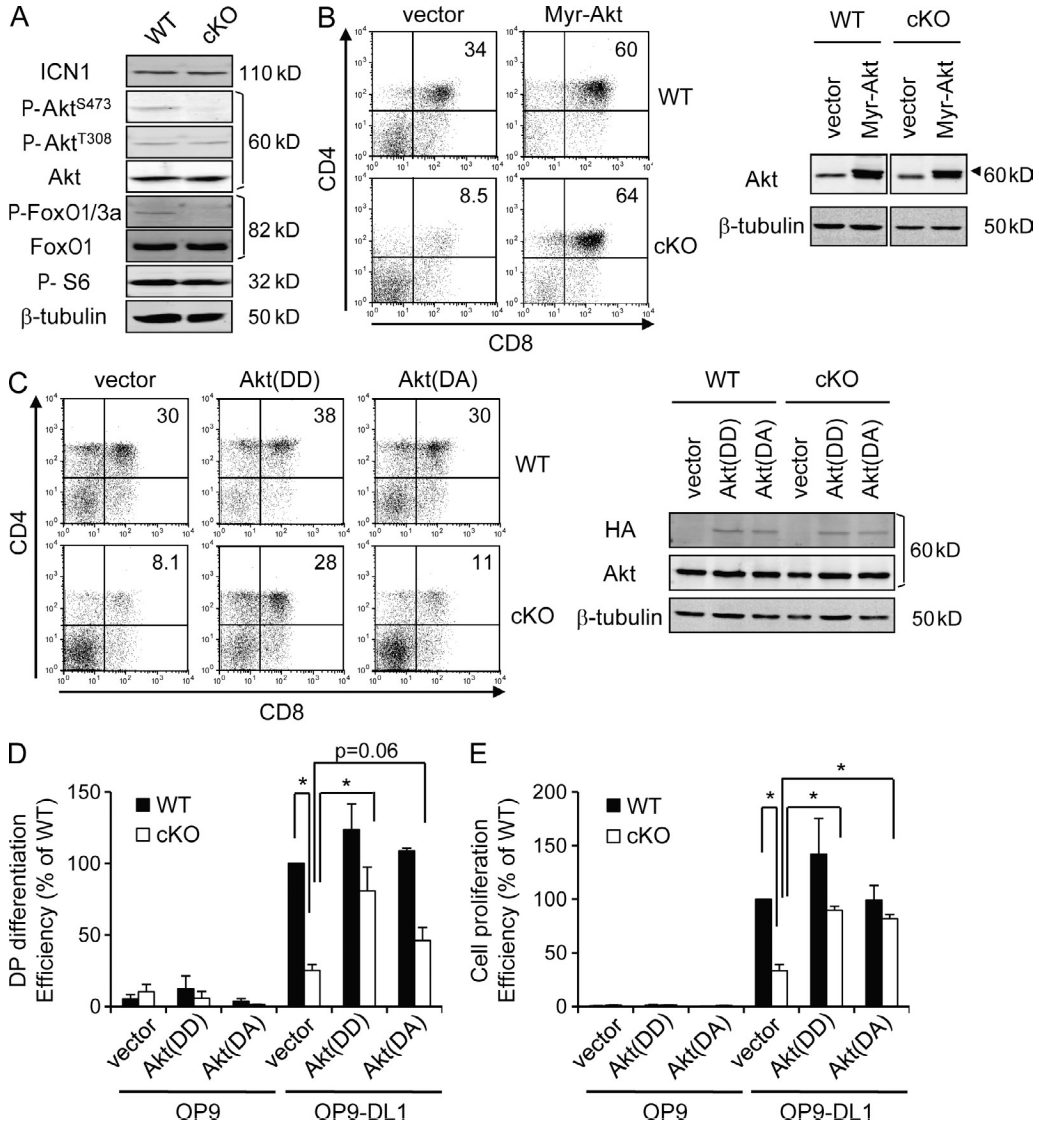

Figure 3. Active Akt is epistatic to *Rictor* in Notch-driven pre-T cell differentiation and proliferation. (A) Purified DN thymocytes cultured for 2 d on OP9-DL1 cells were analyzed by immunoblotting (one result of two independent experiments; cultures of OP9 without DL-1 yield too few cells for these analyses). (B–E) Purified DN cells were cultured for 6 d on OP9-DL1 or OP9, during which time they were transduced with vector, Myr-Akt, Akt(DD), and Akt(DA), and then analyzed. (B and C) Shown are CD4 and CD8 profiles in the viable lymphoid GFP+ gates in one experiment representative of three independent replicates, along with Western blots of Akt or the HA tag on Akt(DD) and Akt(DA), as indicated. Myr-Akt was detected as a band migrating slower than endogenous Akt. (D) Mean (±SEM) efficiency of differentiation into DP thymocytes in the GFP+ gate for the three replicate experiments of B and C, normalized to vector-transduced WT cells grown on OP9-DL1. *, $P < 0.05$. (E) Mean (±SEM) population increases, with normalization and replicates as in D. *, $P < 0.05$.

Evidence that the rictor effect on DN thymocytes involves concerted actions of the NF-κB and FoxO pathways

To explore the respective contributions of the FoxO1/3a and NF-κB pathways, we first tested whether excess FoxO could impact DN cells cultured on OP9-DL1. Lack of phosphorylation of FoxO1/3a impairs their 14-3-3 protein-mediated egress from nuclei. This failure should be phenocopied by use of FoxO3(AAA), a FoxO mutant with alanine substitutions at the kinase target sites (Nakamura et al., 2000; Waugh et al., 2009). When DN thymocytes were transduced with this FoxO mutant, a substantial decrease in proliferative expansion of the pre-T cells compared with controls was observed (Fig. 5 A), so we next tested whether decreasing FoxO1/3a could reverse the impairment of rictor-deficient cells. An RNA interference (RNAi)–driven decrease in FoxO1 and FoxO3 led to a very modest but reproducible improvement in the efficiency of DP differentiation in the cultures (Fig. 5 B) and enhanced the multiplication of *Rictor* cKO thymocytes (Fig. 5 C). In contrast, neither proliferation nor differentiation was increased by transduction of IKK2(SSEE) (Fig. 5, B and C), an IKK2 mutant with phosphomimetic mutations at its T loop activating residues and constitutive activity (Fig. 5 D; Carter et al., 2001). Strikingly, the combination of IKK2(SSEE) with reduction of FoxO1 and FoxO3 by RNAi reproducibly promoted increases in both the prevalence and yield of DP products (Fig. 5 B). The inability to restore complete normalcy indicates that yet further targets downstream from mTORC2 and Akt remain to be identified. Nonetheless, these findings provide evidence that the FoxO and classical NF-κB signaling pathways collaborate to promote the DN to DP conversion downstream from mTORC2.

Role of mTORC2 in T lineage ontogeny

We next examined whether rictor depletion in DN thymocytes resulted in any alteration of the T lineage in vivo. Both $CD4^+$ and $CD8^+$ T cell numbers were reduced in the

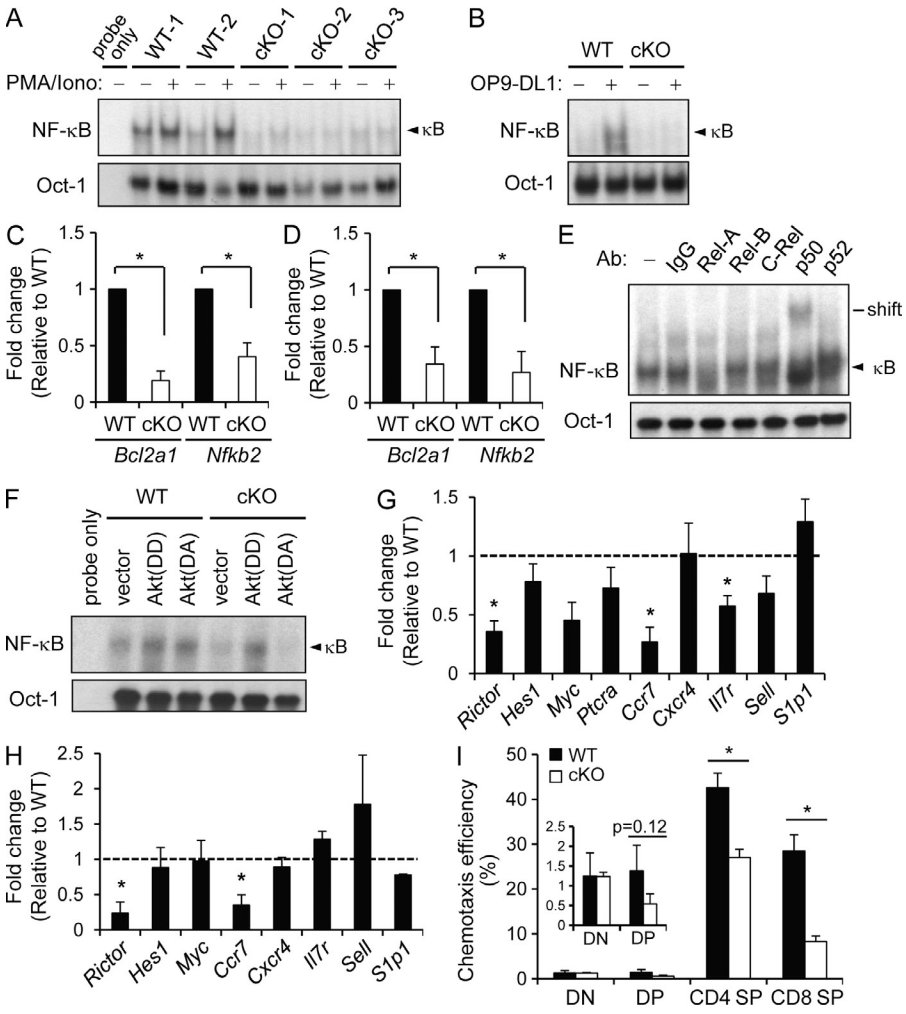

Figure 4. Notch-induced NF-κB requires mTORC2. (A) Nuclear extracts prepared from thymocytes of individual mice were analyzed by EMSA for nuclear NF-κB. Binding of the Oct-1 transcription factor was used as a loading control. (A, B, and E: one result is shown, representative of two independent experiments.) (B) Purified $CD4^-CD8^-$ thymocytes were analyzed by EMSA for nuclear NF-κB after 2-d culture on OP9 or OP9-DL1 cells in the presence of IL-7. (C and D) RNA isolated from purified DN thymocytes (C) or $CD4^-CD8^-$ cells (D) cultured for 2 d on OP9-DL1 cells was analyzed by qRT^2-PCR for NF-κB target genes. Shown are the mean (±SEM) concentrations of mRNA in cKO relative to WT, averaging five (C) and two (D) independent replicate experiments. *, $P < 0.05$. (E) Nuclear extracts of WT DN thymocytes cultured for 2 d on OP9-DL1 (B) were analyzed by EMSA for nuclear NF-κB after incubation with antibodies (Ab) against the indicated NF-κB/Rel proteins or nonimmune IgG control. (F) Purified DN thymocytes were transduced with vector, Akt(DD), and Akt(DA) while cultured on OP9-DL1 cells for 2 d. EMSAs were performed using nuclear proteins of transduced cells after purifying $Thy1.1^+$ cells. Of two independent experiments, one result is shown. (G and H) Effects on target genes in *Rictor*-null thymocytes. RNA isolated from purified DN thymocytes (G; five independent experiments) or DN cells cultured for 2 d on OP9-DL1 (H) were analyzed by qRT^2-PCR. As in C and D, mean (±SEM) values for the ratios of expression in *Rictor* cKO samples, each compared with WT in the same replicate experiment, are shown (H: two biologically independent experiments, each in duplicate). *, $P < 0.05$. (I) *Rictor*-null thymocyte chemotaxis to CCL19, a CCR7 ligand. Shown are mean (±SEM) values for WT and cKO thymocytes, averaging two independent experiments, each with duplicate samples, after enumeration and flow cytometric subset determination. *, $P < 0.05$.

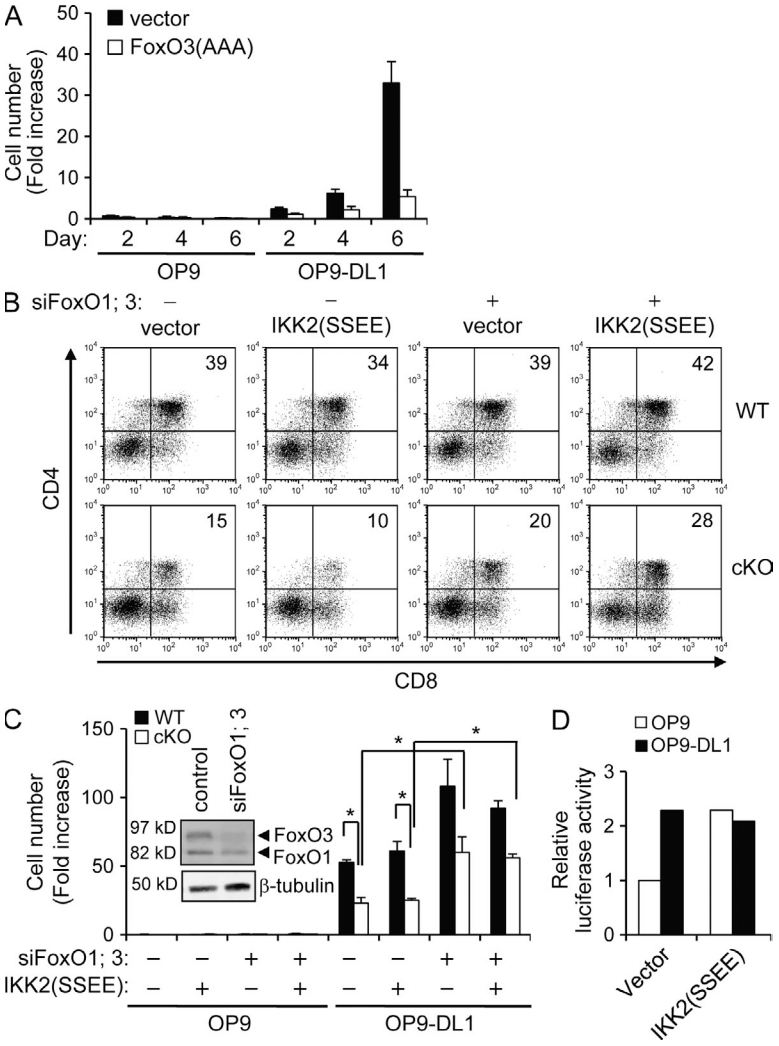

Figure 5. Actions of the NF-κB and FoxO pathways downstream from mTORC2. (A) Cell multiplication was measured as in Fig. 3 E after purified DN thymocytes were transduced with pBMN-vector or pBMN-FoxO3(AAA) and cultured on OP9 cells ± DL1. Shown are the fold increases in cell numbers for the indicated periods (mean ± SD; two replicate experiments, each performed in duplicate). (B and C) DN thymocytes nucleofected with siRNAs for FoxO1 and FoxO3a were transduced with vector or IKK2(SSEE), cultured for 6 d on OP9-DL1, and then analyzed as in Fig. 3 (C–E). Shown are CD4 and CD8 profiles for viable lymphoid cells in the Thy1.1$^+$ gate (B), with inset numbers showing the percentage of DP cells produced by the culture, and fold increase in cell number (C; representative data from B or mean ± SEM of the replicates in C; three separate experiments). The inset shows immunoblots of FoxO1 and FoxO3 in thymocytes after nucleofection for RNAi. *, $P < 0.05$. (D) NF-κB activity in IKK2(SSEE)-transfected thymocytes. Purified DN thymocytes were nucleofected with TK-Renilla luciferase, RE/AP-luciferase, and MiT-IKK2(SSEE) or its vector control and then cultured for 2 d on OP9 cells ± DL1. Shown are luciferase activities normalized for transfection efficiency (one luciferase assay result, representative of two separate experiments).

spleen and lymph nodes of cKO mice (Fig. 6, A and B). Homeostatic expansion driven by T cell underproduction leads to increased frequencies of CD44^{hi} cells, and the prevalence of CD44^{hi} and CD25$^+$ T cells was much higher among the peripheral T cells of cKO mice as compared with WT controls, especially for CD8$^+$ T cells (not depicted). These findings suggested that thymic development was reduced and that mTORC2 function during thymocyte ontogeny is essential for normal populations of conventional T cells. Consistent with this, cKO mice had reduced thymic cellularity (Fig. 6 C and Table 1). Because the Notch-driven proliferation and differentiation of DN into DP cells depended on mTORC2 in the OP9-DL1 system, we quantitated thymocyte subpopulations. Cell numbers in each major thymocyte subset were reduced in *Rictor* cKO animals, but it was notable that the prevalence of DN thymocytes increased while that of their DP descendants decreased (Fig. 6, D–F). This finding provides evidence that the efficiency of this developmental transition in situ was reduced by Rictor deficiency, consistent with the findings with OP9-DL1 cultures. Together, the results indicate a requirement for mTORC2 in achieving normal rates of developmental progression in T cell ontogeny.

DN thymocytes can be further subdivided on the basis of CD44 and CD25 expression. For analyses of these DN subsets, we used both the *Lck*-Cre transgene and, to complement these results, a *Vav*-Cre transgene (Table 1) that drives deletion before specification of T lineage fate (de Boer et al., 2003). Increases in CD44$^-$CD25$^+$ DN3 cells relative to their CD44$^-$CD25$^-$ DN4 successors were observed in thymi made *Rictor* null by each method (Fig. 6, G and H), suggesting an impaired DN3/DN4 transition. Notch signaling directs and then cements a T lineage fate at the DN1 and DN2 stages (Schmitt et al., 2004), so it was intriguing that a decrease in DN1 cells also was observed (Fig. 6, G and H). We further analyzed the cell-intrinsic impairment of thymocyte ontogeny analyzing the competitive fitness of Rictor-deficient thymocytes developing together with WT counterparts in vivo. After transfer of bone marrow from WT or cKO mice along with fixed portions of marrow from allotypically disparate WT mice, marrow reconstitution was equivalent (not depicted), but the fitness of WT T lineage cells within the thymus was ~16-fold greater than that of mTORC2-deficient counterparts generated using the *Vav*-Cre transgene (Fig. 7, A and B). Detailed thymocyte subset analyses showed the decrease in DN1 rictor-deficient cells and impediment to progression to a DP stage (Fig. 7, C–E). We conclude that Rictor is required in cell-autonomous processes of normal T cell development in the thymus, both in establishing normal numbers of cells and in promoting the DN to DP transition.

The findings suggesting a defect of proliferative expansion led us to measure the effect of Rictor deficiency on thymocyte

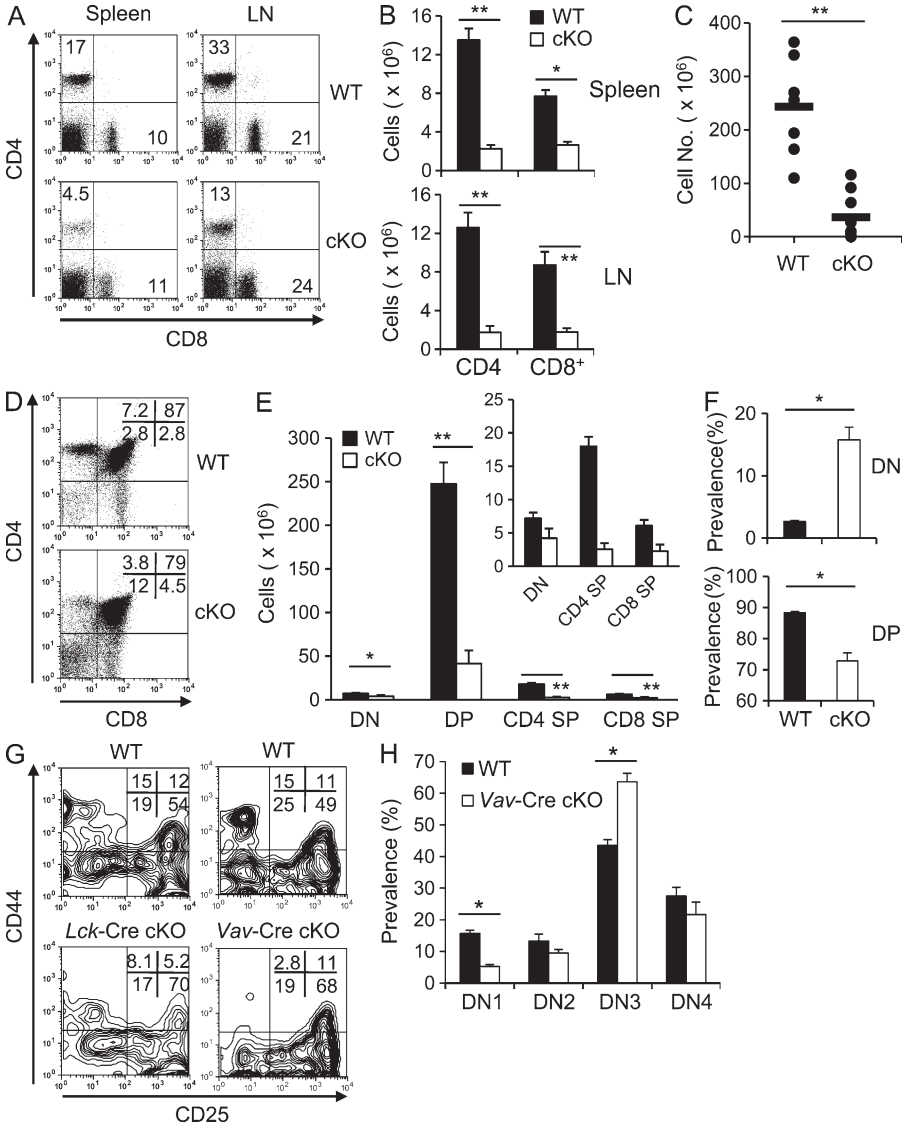

Figure 6. Normal T cell development and thymocyte progression require Rictor. Representative or mean (±SEM) data ($n = 9$ for each genotype) are shown. (A and B) Spleen and lymph node cells of 5–6-wk-old *Lck*-Cre, *Rictor*$^{fl/fl}$ mice versus WT controls. (A) Flow cytometry analyses, with frequencies (%) of CD4$^+$ and CD8$^+$ T cells presented as inset numbers (A), and T cell numbers from peripheral lymphoid organs (B). (B, C, E, and F) Shown are the mean (±SEM) calculated numbers of cells in the indicated subsets from spleen and pooled lymph nodes (B) or thymi (C, E, and F) of nine mice per genotype. *, $P < 0.05$; **, $P < 0.01$. (C–G) Thymocyte populations in cKO mice. (C) Thymic cellularity. Horizontal bars indicate the mean cell number. (D and E) Thymocyte subsets of the same *Lck*-Cre, *Rictor*$^{fl/fl}$ and WT mice as for A–C were determined using CD4 and CD8; numbers were calculated using cellularity of each thymus. (E [inset] and F) The same data plotted on a scale facilitating comparisons for DN and single-positive (SP) populations. Shown are the mean (±SEM; $n = 9$) calculated numbers of cells in the indicated subsets. (G) DN thymocytes of the same *Lck*-Cre, *Rictor*$^{fl/fl}$ and WT mice as for A–F or a separately matched cohort of *Vav*-Cre, *Rictor*$^{fl/fl}$ mice and WT controls ($n = 8$ for each genotype) were categorized into DN1–DN4 subsets by flow cytometry for CD25 and CD44 (DN1, CD44^{hi}CD25$^-$; DN2, CD44^{hi}CD25$^+$; DN3, CD44^{lo}CD25$^+$; and DN4, CD44^{lo}CD25$^-$). Shown are representative flow cytometric profiles of these markers on DN thymocytes of WT, *Lck*-Cre cKO, and *Vav*-Cre cKO, with insets showing the prevalence (%) in each quadrant (B) and mean frequencies (%) of the DN subsets. (H) Mean (±SEM) DN1–DN4 frequencies for the cohort ($n = 8$ each) of *Vav*-Cre cKO versus WT mice. *, $P < 0.05$.

proliferation. BrdU incorporation after a short-term pulse showed DN thymocytes (especially DN4 cells) of WT mice to be highly proliferative in vivo (Fig. 7 F). In contrast, frequencies of BrdU$^+$ cells in each postexcision DN subset were reduced in cKO mice. Rates of proliferation after stimulation in vitro were similarly reduced for the Rictor-deficient thymocytes, but their apoptosis was not affected by lack of mTORC2 (not depicted). The metabolic defects and block to DN4 progression caused by PDK1 deletion in thymocytes were associated with dramatically lower expression of several trophic receptors (Kelly et al., 2007). However, as in the results of cultures on OP9-DL1, PDK2 deficiency of *Rictor* cKO thymocytes led to only a very modest reduction of the transferrin receptor CD71 (not depicted), and mTORC2-deficient DN thymocytes were of normal cell size (measured by FSC; not depicted) and glycolytic rate (Fig. 7 G). We infer that mTORC2 contributes to the production of a full T cell complement by promoting thymocyte proliferation.

mTORC2 facilitates Notch-driven T-ALL development

Physiological Notch signaling organizes developmental fates, yet gain of function mutations in *Notch1* are common in cancer. More than 50% of the human T-ALL cells depend on ongoing Notch-initiated signals for their growth or viability (Weng et al., 2004). Accordingly, we tested the impact of Rictor on Notch-induced T-ALL using a mouse model in which hematopoietic bone marrow precursors were transduced to express the Notch1 cleaved intracellular polypeptide (ICN1) and transplanted into recipient mice. As expected, Thy1$^+$ CD4$^+$CD8$^+$ cells arose in the bone marrow and entered the circulation by 2 wk after transplantation. Stochastic malignant transformation was then followed by tissue invasion and death. Whereas at most a modest impact of mTORC2 deficiency on circulating Thy1$^+$ CD4$^+$CD8$^+$ could be detected, median survival almost doubled when donor marrow was programmed to delete rictor (Fig. 8, A–C). To explore the improvement in survival despite an equivalent emergence

Table 1. Cellularity of thymi and spleens of *Vav*-Cre *Rictor*$^{fl/fl}$ mice

Cell type	WT	*Vav*-Cre *Rictor*$^{fl/fl}$
Total thymocytes	237 ± 11	80 ± 12[a]
DN thymocytes	7.1 ± 0.5	5.3 ± 0.8[a]
DP thymocytes	206 ± 9.9	65 ± 11[a]
CD4 SP thymocytes	16 ± 1.0	4.8 ± 0.9[a]
CD8 SP thymocytes	7.6 ± 0.4	5.4 ± 0.8[a]
Total splenocytes	98 ± 10	37 ± 4.5[a]
CD4$^+$ splenocytes	15 ± 1.7	4.6 ± 0.3[a]
CD8$^+$ splenocytes	10 ± 1.0	3.6 ± 0.4[a]

SP, single positive. Mean ± SEM ×10^6 cells is shown.
[a]$P < 0.05$.

of the preleukemic or leukemic cells in bone marrow and blood, we analyzed organ infiltration. Leukemic cells in liver, lung, and kidney were strikingly decreased by the *Rictor* loss of function mutation (Fig. 8 D). Expression of NF-κB target genes (*Bcl2a1* and *Nfkb2*) were significantly decreased in the cKO T-ALL, whereas selected FoxO target genes (*Il7ra*, *Sell*, and *S1p1*) were not (Fig. 8 E). The NF-κB–dependent chemokine receptor CCR7 has been reported as an important determinant of Notch-induced T-ALL pathogenesis and death because of a necessary and sufficient role in trafficking of the leukemic cells into tissue (Hasegawa et al., 2000; Jongen-Lavrencic et al., 2005; Buonamici et al., 2009), and *Ccr7* expression by mTORC2-deficient thymocytes was greatly reduced. Strikingly, circulating GFP$^+$ Thy1$^+$ cells from recipients of Notch-driven marrow programmed to delete *Rictor* showed significant decreases in *Ccr7* gene expression (Fig. 8 E) while confirming the loss of *Rictor* mRNA. Moreover, deaths from leukemia were slower with Rictor-deficient cells after transfers of equal numbers of WT or cKO leukemic cells into irradiated recipients (Fig. 8 F). All together, this study provides evidence that PDK2 activity of mTORC2 is an important determinant of the capacity of Notch to induce NF-κB and CCR7, as well as accelerated tissue invasion and death in T-ALL.

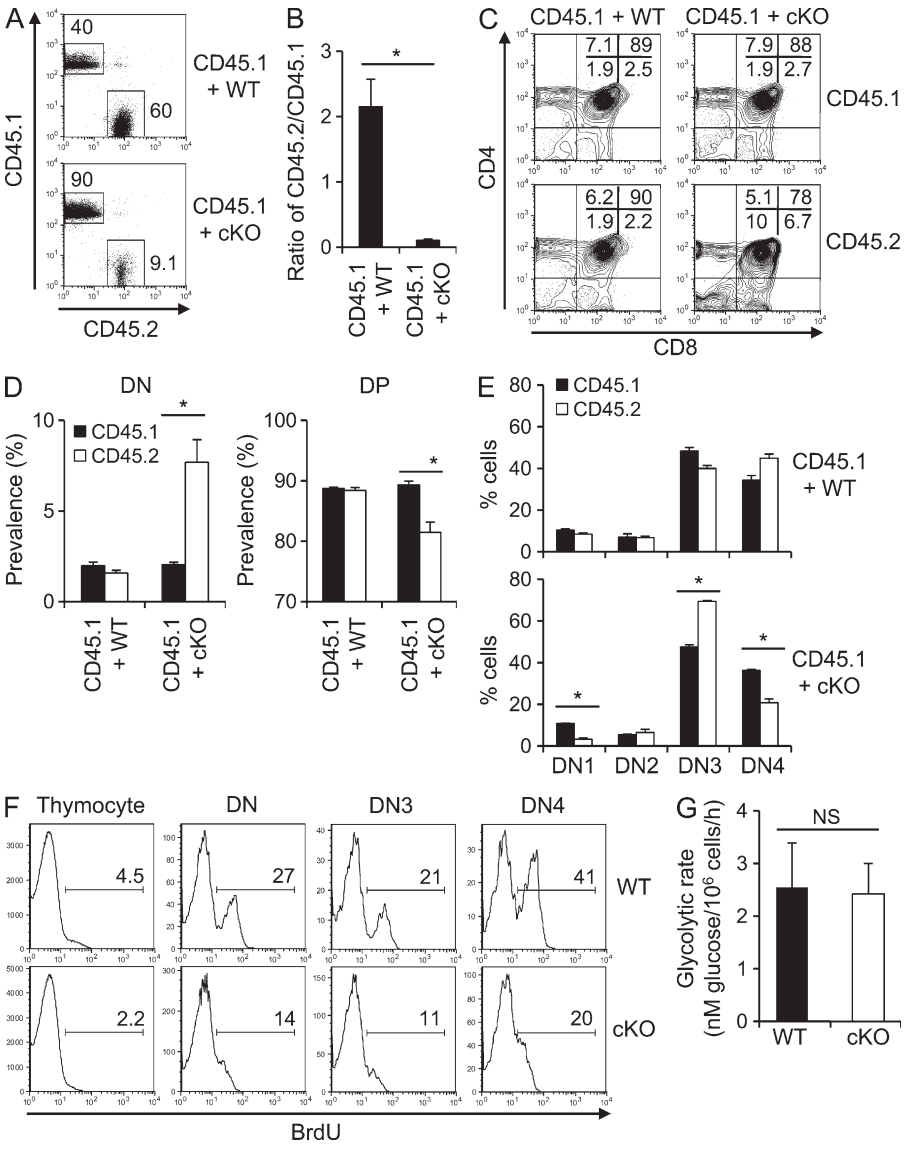

Figure 7. Defects of *Rictor*-null thymocyte development are cell autonomous. (A–E) Thymocytes were analyzed 2 mo after transplanting equal numbers of bone marrow cells from WT or *Vav*-Cre cKO mice (CD45.2) mixed with constant fractions of allotypically disparate (CD45.1) WT marrow cells and transferred into irradiated CD45.1 recipients. Shown are CD45.1 and CD45.2 profiles from one representative sample pair in one experiment representative of two replicates (A and C) and the mean (±SEM) ratios of test cells (CD45.2)/internal WT standards (CD45.1; B), averaging the samples of the two independent experiments (B, D, and E), comparing three versus three or two versus two recipients of WT versus cKO CD45.2 marrow. *, $P < 0.05$. (C–E) Within the CD45.1$^+$ and CD45.2$^+$ gates of B, CD4 and CD8 profiles (C), mean (±SEM) prevalence of DN and DP populations (D), and mean (±SEM) frequencies of DN subsets 1–4 (E). (F) Thymocytes were analyzed by flow cytometry after injection of BrdU into WT and *Vav*-Cre *Rictor* cKO mice. Shown are representative histograms from one of three independent experiments with the same results. Numbers denote the percentage of BrdU$^+$ cells in the indicated gates (DN, CD4$^-$CD8$^-$; DN3, CD44^{lo}CD25$^+$; and DN4, CD44^{lo}CD25$^-$ in the DN gate). (G) Normal glycolytic rate of Rictor-null thymocytes. Shown are mean (±SEM) data, averaging results of two independent experiments using five Lck-Cre versus five matched WT controls.

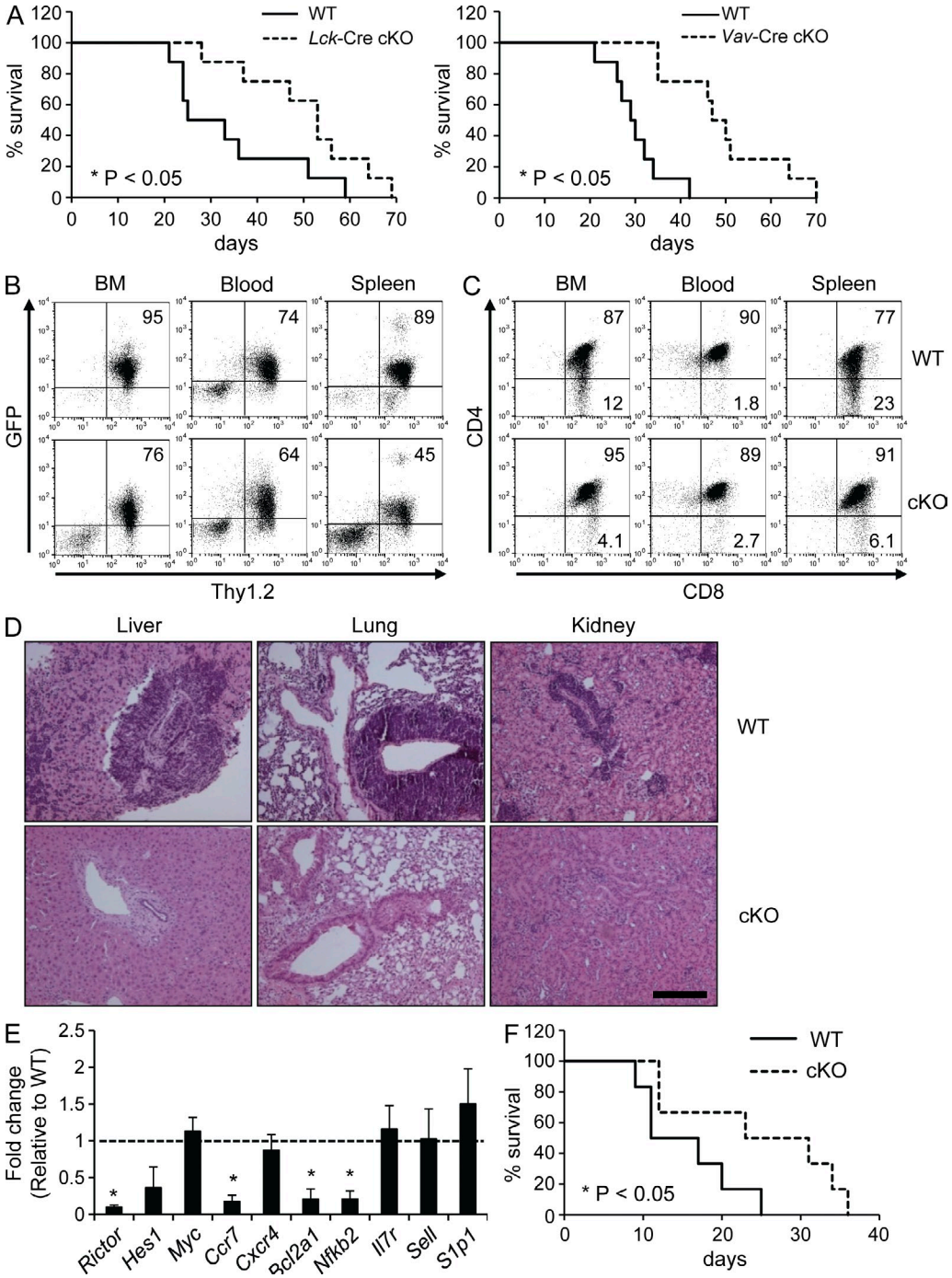

Figure 8. mTORC2 facilitates Notch-induced T-ALL. (A) Shown are the Kaplan-Meyer survival curves for recipient mice after transplantation of ICN1-transduced bone marrow progenitors of WT and cKO mice. (left) Cohorts using marrow of *Lck*-Cre$^+$, *Rictor*$^{fl/fl}$ mice or littermate WT (Cre$^-$) controls (n = 8 vs. 8). (right) Cohorts using marrow of *Vav*-Cre$^+$, *Rictor*$^{fl/fl}$ mice or littermate WT controls (n = 8 vs. 8; for each cohort, $P < 0.05$ by statistical analysis as in Materials and methods, and $P < 0.05$ in statistical test of merged data of the two separate cohorts of cKO vs. WT). (B and C) Engraftment and leukemic cell characteristics. Shown are representative flow cytometry results for Thy1 and GFP (B) of bone marrow, spleen, and blood mononuclear cells (WT vs. cKO donor marrow) at 4 wk after transplantation, along with the CD4 and CD8 profiles of the same GFP$^+$ Thy1.2$^+$ gated cells (C). Shown are results from one representative mouse of WT versus cKO donor marrow (from data on >10 recipients of WT marrow and >10 cKO; >5 pairs for each Cre genotype), with the same results being obtained with marrow from *Lck*-Cre (n > 5 vs. > 5) and *Vav*-Cre (n > 5 vs. > 5) donor series. (D) Hematoxylin and eosin staining of liver, lung, and kidney sections from representative leukemic mice 4 wk after transplantation (sample spectrum and numbers as for C). Bar, 50 µm. (E) qRT^2-PCR analyses of a subset of Notch, NF-κB, and FoxO target genes. Shown are fold changes (±SEM) relative to WT leukemic cells (Thy1.2$^+$ cells) isolated from recipient spleen (n = 3 vs. 3). *, $P < 0.05$. (F) Leukemic cells isolated 4–6 wk after transplantation of ICN1-transduced progenitors were transferred into irradiated B6.PL-Thy1a recipients (5×10^5 GFP$^+$ Thy1.2$^+$ cells each). Shown are the Kaplan-Meyer survival curves merged from two independent transfers, each with three versus three recipients, after transfer of leukemic cells stemming from WT or *Vav*-Cre cKO marrow progenitors.

DISCUSSION

Steps in the early thymic development of T cells are critically regulated by Notch in collaboration with other signals (Maillard et al., 2005). The evidence presented here shows that T lineage cells require an intact mTORC2 to fully execute biological effects that are driven by Notch. Pre-T cell proliferation and differentiation efficiency were impaired by loss of the gene encoding an essential subunit of mTORC2, and Akt and NF-κB activities were diminished both in situ and in an experimental model driven by increased Notch engagement. NF-κB activity and biological outcomes required mTORC2 in an experimental context where other stimuli that also impact PI3K-related or NF-κB signaling (OP9-derived factors; IL-7; pre-TCR; etc) were comparable. Of note, a kinase that is a direct mTORC2 target mitigated key defects (NF-κB levels, pre-T cell proliferation, and DP differentiation), providing evidence that the findings are caused by mTORC2 rather than an alternative function of Rictor. The data suggest that Akt-dependent NF-κB activity is important in relation to CCR7 expression and leukemia cell localization. Collectively, these findings provide genetic evidence for vital roles of *Rictor* and mTORC2 in developmental and pathological effects of Notch, complementing previous indications that mTORC1 participates in these processes (Luo et al., 1994; Janes et al., 2010; Tandon et al., 2011).

Rapamycin causes significant thymic atrophy by repressing growth and proliferation of thymocytes (Luo et al., 1994), and mTOR is the known enzymatic target of this pharmaceutical agent (Laplante and Sabatini, 2009). However, little is known about relative roles of the two classes of mTOR complex in thymic T cell development, or in the context of Notch signaling or Notch-initiated pathologies. Only mTORC1 is acutely inhibited by rapamycin because of its Raptor subunit, but chronic administration of rapamycin over time led to impairment of Akt(S473) phosphorylation (Sarbassov et al., 2006; Lee et al., 2010; Delgoffe et al., 2011). Thus, the chronic effects of rapamycin on the thymus might be attributable either to mTORC1, mTORC2, or both. The finding that mTORC2 depletion impaired thymocyte numbers and created a bottleneck impairing the efficiency of DN to DP differentiation, together with work indicating that a week of in vivo rapamycin treatment eliminated phosphorylation of Akt S473 (Sarbassov et al., 2006), suggests that at least some of the rapamycin effect can be attributed to mTORC2. The need for mTORC2 in execution of a Notch-initiated signal and the thymic phenotype of *Lck*-Cre, *Rictor*$^{fl/fl}$ mice parallel the results with mice in which the main transcriptional target of all four Notch proteins, RBP-J, was deleted using the same Cre transgene. In this work (Tanigaki et al., 2004), DN thymocyte numbers decreased substantially because of a defect of the proliferative burst, and a bottleneck in the DN to DP transition similar to that of mTORC2-deficient thymocytes was present.

Nonetheless, both mTOR complexes probably play a role downstream from Notch. First, the distortion of the DN to DP ratio was greater in RBP-J–deficient mice than the *Rictor* cKO. Second, phosphorylation of the mTORC1 target residue in p70 S6K decreased after treatment of human T-ALL cells with a γ-secretase inhibitor (Chan et al., 2007). Moreover, ablation of one p70 S6K isoform, S6K1, caused a modest delay in the onset of leukemia initiated by conditional loss of *Pten* (Tandon et al., 2011). In this regard, it is intriguing that in PTEN-deficient prostate cancer cells, the activity of Akt influenced the NF-κB pathway by driving an association of Raptor with IKK-α (Dan et al., 2008). This study is compatible with the present results because mTORC2 enhanced Akt activity and thus may be upstream from the Raptor-IKK mechanism in some settings. Finally, although our data reveal mTORC2 function as a precondition for full Notch signaling in leading to the DP stage, *Rictor* may also act at Notch-independent steps later in ontogeny (Tanigaki et al., 2004; Delgoffe et al., 2011).

Notch stimulates glycolysis, glucose uptake, and nutrient receptor expression by pre-T cells, thereby promoting the survival, growth, and differentiation of these cells (Ciofani and Zúñiga-Pflücker, 2005). The findings with mTORC2 depletion provide evidence that glycolysis and nutrient receptor expression can be dissociated from a strong growth and differentiation phenotype, as these metabolic parameters were normal in Rictor-deficient thymocytes yet DL1-stimulated proliferation and co-induction of CD4 and CD8 were impaired. Previous work showed that these trophic responses to Notch depend on PDK1 (Kelly et al., 2007). Thus, when the *Lck*-Cre transgene was used for cell type–specific inactivation of the *Pdk1* gene, cell size, survival, and CD71 expression were all dramatically decreased, along with an almost complete block in the DN to DP transition (Kelly et al., 2007). Both PDK1 and mTORC2 target Akt as a major downstream effector, but our data reveal several differences from the PDK1 effects on pre-T cells. In contrast to early PDK1 deficiency, rictor depletion did not substantially affect cell size, CD71 expression, or glycolytic rate in thymocytes or DN cells cultured on OP9-DL1. Thus, mTORC2 and its phosphorylation of Akt S473 appear dispensable for the Notch-induced trophic signaling in thymocytes. In addition to Akt, PDK1 phosphorylates and activates multiple AGC family kinases (S6K1, RSK, and PKC isoforms; Collins et al., 2003), and the capacity to activate NF-κB via TCR signaling also depends on PDK1 (Lee et al., 2005). A genetic approach that replaced WT PDK1 with a mutant enzyme supporting activation of Akt but not other AGC kinases did not restore thymocyte numbers despite normalizing nutrient receptor expression on pre-T cells (Kelly et al., 2007). Collectively, then, Notch and PDK1 require more than Akt activity alone when considering signaling at physiologically meaningful levels, but our findings imply that normal thymocyte progression requires a threshold level of Akt activity.

In this regard, it is intriguing that the functional consequences of defective PDK2 activity analyzed here may also indicate a role for signal relays in addition to Akt under physiological conditions. Although Myr-Akt transduction into Rictor-deficient DN thymocytes was able to drive cultures on OP9-DL1 to yield as many DP cells as were obtained

with the Myr-Akt–transduced WT cells, epistasis with the more physiological Akt mutant, Akt(DD), led only to numbers equivalent to vector-transduced WT cells. Because PKC isoforms are targets of mTORC2 kinase activity (Facchinetti et al., 2008; Ikenoue et al., 2008; Lee et al., 2010), it is attractive to speculate that the PKCs expressed in developing thymocytes need to be sufficiently active unless Akt activity is at the very high level achieved by Myr-Akt. Pre-TCR signaling leads to activation of the NF-κB pathway in thymocytes to facilitate survival (Voll et al., 2000), so it is likely that the increased Akt activity caused by HM phosphorylation operates in part through NF-κB. However, our findings also indicate that Akt phosphorylation of FoxO proteins amplifies DN thymocyte proliferation. This mechanism would mirror the model inferred for regulation of the T reg cell fate choice at later stages in the T lineage, i.e., Akt regulation of FoxO proteins whose binding to regulatory chromatin at the *Foxp3* locus is vital for induction of FoxP3 expression (Harada et al., 2010; Ouyang et al., 2010).

In addition to observing defects in Notch-induced pre-T cell proliferation and differentiation, Rictor depletion substantially prolonged survival in the setting of extreme Notch drive leading to death from leukemia. In this model of T-ALL, the cancer preferentially arises from pre-T type cells to evade an Ink4a/Arf-imposed restriction (Volanakis et al., 2009; Medyouf et al., 2010), but there are several phases of leukemic cells across time after bone marrow transfer (Campese et al., 2006). The initial emergence of abnormal GFP^+ cells into blood and their rising prevalence over time were similar in recipients of WT and cKO marrow, whereas disease was still delayed upon secondary transfer of leukemic cells into new recipients. These findings suggest that the protective effect of mTORC2 deficiency in this setting was exerted at a later step in oncogenic progression or disease. Of note, mTORC2 transduced signals that regulate expression of the NF-κB–dependent *Ccr7* gene in the leukemic cells, extending the insight that mortality from ICN1-induced T-ALL depended on CCR7-mediated chemotaxis into tissues (Buonamici et al., 2009). Our evidence that NF-κB activity and expression of other NF-κB target genes (*Nfkb2* and *Bcl2a1*) are reduced in the *Rictor* cKO cells indicates that NF-κB transcription factors are likely to be key mediators of the mTORC2 contribution to T-ALL in this setting. The findings with transduction of constitutively active Akt mutants into the impaired *Rictor* cKO thymocytes indicate that this kinase can suffice to drive a restoration of NF-κB activity. However, mTORC2 was also found to be important for regulation of the amount of *Hes1* mRNA induced by Notch. In light of evidence that Hes1 appears to serve as a direct repressor of *Cyld* (*Cylindromatosis*) gene expression, with CYLD in turn inhibiting NF-κB pathway activity, the Akt impact on NF-κB and T-ALL may involve collaboration of Akt with other signaling components (Espinosa et al., 2010).

Central challenges facing chemotherapy for T-ALL or other Notch-dependent tumors (Ranganathan et al., 2011) include the dose-limiting toxicities of γ-secretase and perhaps other Notch inhibitors (Searfoss et al., 2003; Real and Ferrando, 2009), the different structures and functions of the mTOR signaling complexes, and the inherent capacity of mTORC1 inhibitors to increase PI3K signal initiation as the result of relief of negative feedback at an apical level (Bhaskar and Hay, 2007; Guertin and Sabatini, 2009). Using enzymatic inhibitors of both mTOR complexes, or of mTOR and PI3K, offers new promise (Real et al., 2009; Carayol et al., 2010; Chiarini et al., 2010; Janes et al., 2010; Altman et al., 2011). The genetic evidence that Rictor deficiency protects against T-ALL, independent from apparent changes in mTORC1 activity, supports the need to block mTORC2. In addition, the finding suggests that more selective inhibition of mTORC2 might offer an independent therapeutic approach with lower inherent toxicities.

MATERIALS AND METHODS

Mice and bone marrow transplantation. (B6 × 129S/v) $Rictor^{fl/fl}$ mice (Shiota et al., 2006) were bred to a B6 (C57BL/6-J) background and crossed with transgenic mice (C57BL/6) expressing Cre recombinase under control of the proximal *Lck* promoter (*Lck-Cre*; $n \geq 4$ for *Rictor* backcrosses to B6) or *Vav1* promoter (*Vav-Cre*; $n \geq 6$), and PCR genotyping was performed as described previously (Lee et al., 2010). All mice were housed in individually ventilated micro-isolator cages in specific pathogen–free conditions and used as monitored by the Vanderbilt University Office of Animal Welfare Assurance after approval of experimental protocols by the Institutional Animal Care and Use Committee. Because of evidence of a substantial heterozygote phenotype and no evidence of an impact of the Cre transgenes on $Rictor^{+/+}$ cells, experiments were performed either comparing Cre^- littermate controls with Cre^+ $Rictor^{fl/fl}$ mice or, for further validation, parallel genetic stock at similar backcross generations but Cre^+ $Rictor^{fl/fl}$ versus Cre^+ $Rictor^{+/+}$. For mixed competitive chimeras, bone marrow cells were obtained from B6 (CD45.2) WT and *Vav*-Cre, $Rictor^{fl/fl}$ as well as B6-CD45.1 mice (ages 6–8 wk). After depletion of T and B lineage cells using microbeads, 4×10^6 $Thy1^-$ $B220^-$ marrow cells were mixed with equal numbers of CD45.1 marrow cells and injected intravenously into lethally irradiated (10 Gy in two divided doses) B6-CD45.1 recipients. For Notch-driven leukemia experiments, bone marrow cells were obtained from mice 4 d after treatment with 150 mg/kg 5-FU (Campese et al., 2006), incubated (2 d) in DME supplemented with 15% FBS, 10 ng/ml IL-3, 20 ng/ml IL-6, and 50 ng/ml stem cell factor, and transduced with MiGR1-ICN1 (provided by W. Pear, University of Pennsylvania, Philadelphia, PA; Aster et al., 2000). Each lethally irradiated B6.Thy1a recipient (prepared as above) received a mixture of 5×10^5 unmanipulated bone marrow cells along with half of the ICN1-transduced cells. Irradiated mice were maintained on water supplemented with amoxicillin for 2 wk after transplantation.

Antibodies and reagents. Cytokines and antibodies against cell surface markers were purchased from BD except for recombinant mouse IL-7 (Leinco Technologies) and biotinylated anti-Thy1.1 (eBioscience). Primary antibodies for immunoblotting were obtained from Cell Signaling Technology except for anti-rictor (Bethyl Laboratories), whereas infrared dye–conjugated second antibodies were obtained from Rockland or LI-COR Biosciences. Anti-CD4 and anti-CD8 magnetic microbeads were obtained from Miltenyi Biotec, and streptavidin-conjugated IMag particles were purchased from BD.

Cell culture. Thymocytes were cultured in complete medium containing 10% FBS and supplemented as described previously (Lee et al., 2010). For in vitro differentiation of DN thymocytes, monolayers of OP9-DL1 and OP9-control cells (provided by S. Cleveland, U. Dave, and J.C. Zúñiga-Pflücker, Vanderbilt University, Nashville, TN; Ciofani and Zúñiga-Pflücker, 2005) were maintained in αMEM (Sigma-Aldrich) supplemented with 15% FBS. $CD4^-CD8^-$ DN subsets were purified from pooled thymocytes by CD8

depletion using biotinylated anti-CD8 and IMag streptavidin particles followed by CD4 depletion using anti-CD4 microbeads and MACS. DN cells (>95–98% pure) were plated on stromal cell monolayers (OP9-DL1 or OP9-control) in the presence of 5 ng/ml IL-7. Harvested cultures were passed through 40-µm filters to remove the stromal cells, counted, and analyzed by flow cytometry.

Measurements of RNA and proteins by immunoblotting. Proteins in cell lysates were prepared and analyzed by immunoblotting with primary antibodies followed by appropriate dye–conjugated second antibodies as described previously (Lee et al., 2010). Data were imaged and quantitated with the Odyssey Infrared Imaging System (LI-COR Biosciences). Using tabulated primer pairs tabulated, RNA levels were measured in duplicate or triplicate by qRT^2-PCR as described previously (Cho et al., 2009).

BrdU incorporation in vivo and flow cytometry analyses. Thymi were harvested 2 h after two injections (0.5 h apart) of mice with 1 mg BrdU in saline by an i.p. route. Cells were surface stained for direct immunofluorescence, processed for detection of intracellular epitopes, and analyzed as described previously (Lee et al., 2010).

Replicates and statistical analyses. Numbers and phenotypes of cells from each type of mice are representative of a minimum of five mice of each type. Differences between sample sets were analyzed statistically using unpaired two-tailed nonparametric tests of significance (Instat; GraphPad Software); interpretations of difference between samples are based on those for which $P < 0.05$. In the figures, *, $P < 0.05$; and **, $P < 0.01$ in comparing mutant samples with WT controls. NS indicates $P > 0.05$. The Kaplan-Meier log-rank test was used to analyze mouse survival data using R (The R Foundation for Statistical Computing).

Glycolysis assays. Triplicates of freshly isolated thymocytes or DN cells cultured on OP9-DL1 or OP9 control cells for 2 d were washed and pulsed (37°C, 1 h) with 10 µCi 5-[^{3}H]glucose. The reaction was stopped with 0.2 N HCl, and ^{3}HOH generation from 5-[^{3}H]glucose was captured by diffusion into a reservoir of H_2O in a tightly sealed scintillation vial. Diffused and undiffused ^{3}H were then measured by liquid scintillation counting.

Nucleofection and retroviral transduction. Retrovector constructs of the Akt(DD), Akt(DA), and IKK2(SSEE) (provided by D. Ballard, Vanderbilt University) were subcloned into MSCV-IRES-GFP (MiG) and MSCV-IRES-Thy1.1 (MiT) after site-directed mutagenesis of cDNA encoding bovine Akt. Retrovirions were collected from cultures of ΦNX ecotropic packaging cells transfected with retrovector plasmids as described previously (Lee et al., 2010), centrifuged (1 h, 2,500 *g*) with thymic DN cells, and cultured with OP9 (±DL1) stromal cells. RNAi was performed by transfection of purified DN thymocytes using pooled si-dsRNA targeting FoxO1 and FoxO3a (500 nM of each pool; Thermo Fisher Scientific), or GFP, and the mouse T cell Nucleofector kit (Lonza) according to the manufacturer's instructions.

Electrophoretic mobility shift assays (EMSAs). Nuclear extracts from thymocytes were prepared as described previously (Lee et al., 2006). NF-κB consensus oligonucleotide (Santa Cruz Biotechnology, Inc.) were labeled with ^{32}P and incubated with 5 µg of nuclear extract proteins at room temperature for 20 min in a binding buffer (10 mM Hepes, pH 7.9, 65 mM NaCl, 1 mM dithiothreitol, 0.2 mM EDTA, 0.02% NP-40, 50 µg/ml poly(dI·dC), and 8% glycerol). Supershift assay was performed by preincubating with antibodies against RelA, RelB, c-Rel, p50, and p52 (Santa Cruz Biotechnology, Inc.) on ice for 2 h. Complexes were resolved by nondenaturing 4% PAGE.

Chemotaxis. Chemotaxis was assayed using the Transwell system containing 5-µm pore size polycarbonate membranes (Corning). Duplicate thymocyte samples (4×10^6 each) were placed in the upper chamber of each well, and 100 nM CCL19 was added to the lower chamber. After 3-h incubation at 37°C, cells were recovered from the lower chamber, counted, and analyzed by flow cytometry. Migrated cells of each subset were calculated as a percentage of their input number.

We gratefully acknowledge L. Heffington for great technical assistance, S. Cleveland and U. Dave for helpful discussions and provision of OP9 (±DL1) cells, the Flow Cytometry Core for assistance with flow cytometry and preparative sorting, provision of plasmid stocks by Addgene, critical reading of the manuscript by and helpful discussions with R. Zent, E. Sebzda, and S. Zinkel, and gifts of or permission to use reagents from W. Pear, J.C. Zúñiga-Pflücker, F. Radtke, C. Guidos, A. Bhandoola, D. Cantrell, D. Ballard, E. Sebzda, A. Weiss, and L. Kane.

This work was initiated with pilot funds from the Vanderbilt-Ingram Cancer Center Support Grant, P30 CA068485, and then supported by R01AI068149, AI077528, and Vanderbilt Institutional Bridge Funds, followed by HL106812. Additional support by university cores was provided via CA068485 and P60 DK020593 to the Diabetes Center.

No author has any competing financial interest.

Submitted: 18 July 2011
Accepted: 7 March 2012

REFERENCES

Altman, J.K., A. Sassano, S. Kaur, H. Glaser, B. Kroczynska, A.J. Redig, S. Russo, S. Barr, and L.C. Platanias. 2011. Dual mTORC2/mTORC1 targeting results in potent suppressive effects on acute myeloid leukemia (AML) progenitors. *Clin. Cancer Res.* 17:4378–4388. http://dx.doi.org/10.1158/1078-0432.CCR-10-2285

Aster, J.C., L. Xu, F.G. Karnell, V. Patriub, J.C. Pui, and W.S. Pear. 2000. Essential roles for ankyrin repeat and transactivation domains in induction of T-cell leukemia by notch1. *Mol. Cell. Biol.* 20:7505–7515. http://dx.doi.org/10.1128/MCB.20.20.7505-7515.2000

Bentzinger, C.F., K. Romanino, D. Cloëtta, S. Lin, J.B. Mascarenhas, F. Oliveri, J. Xia, E. Casanova, C.F. Costa, M. Brink, et al. 2008. Skeletal muscle-specific ablation of raptor, but not of rictor, causes metabolic changes and results in muscle dystrophy. *Cell Metab.* 8:411–424. http://dx.doi.org/10.1016/j.cmet.2008.10.002

Bhaskar, P.T., and N. Hay. 2007. The two TORCs and Akt. *Dev. Cell.* 12:487–502. http://dx.doi.org/10.1016/j.devcel.2007.03.020

Buonamici, S., T. Trimarchi, M.G. Ruocco, L. Reavie, S. Cathelin, B.G. Mar, A. Klinakis, Y. Lukyanov, J.C. Tseng, F. Sen, et al. 2009. CCR7 signalling as an essential regulator of CNS infiltration in T-cell leukaemia. *Nature.* 459:1000–1004. http://dx.doi.org/10.1038/nature08020

Campese, A.F., A.I. Garbe, F. Zhang, F. Grassi, I. Screpanti, and H. von Boehmer. 2006. Notch1-dependent lymphomagenesis is assisted by but does not essentially require pre-TCR signaling. *Blood.* 108:305–310. http://dx.doi.org/10.1182/blood-2006-01-0143

Carayol, N., E.Vakana, A. Sassano, S. Kaur, D.J. Goussetis, H. Glaser, B.J. Druker, N.J. Donato, J.K. Altman, S. Barr, and L.C. Platanias. 2010. Critical roles for mTORC2- and rapamycin-insensitive mTORC1-complexes in growth and survival of BCR-ABL-expressing leukemic cells. *Proc. Natl. Acad. Sci. USA.* 107:12469–12474. http://dx.doi.org/10.1073/pnas.1005114107

Carpten, J.D., A.L. Faber, C. Horn, G.P. Donoho, S.L. Briggs, C.M. Robbins, G. Hostetter, S. Boguslawski, T.Y. Moses, S. Savage, et al. 2007. A transforming mutation in the pleckstrin homology domain of AKT1 in cancer. *Nature.* 448:439–444. http://dx.doi.org/10.1038/nature05933

Carter, R.S., B.C. Geyer, M. Xie, C.A. Acevedo-Suárez, and D.W. Ballard. 2001. Persistent activation of NF-κ B by the tax transforming protein involves chronic phosphorylation of IkappaB kinase subunits IKKbeta and IKKgamma. *J. Biol. Chem.* 276:24445–24448. http://dx.doi.org/10.1074/jbc.C000777200

Chan, T.O., and P.N. Tsichlis. 2001. PDK2: a complex tail in one Akt. *Sci. STKE.* 2001:pe1. http://dx.doi.org/10.1126/stke.2001.66.pe1

Chiarini, F., C. Grimaldi, F. Ricci, P.L. Tazzari, C. Evangelisti, A. Ognibene, M. Battistelli, E. Falcieri, F. Melchionda, A. Pession, et al. 2010. Activity of the novel dual phosphatidylinositol 3-kinase/mammalian target of rapamycin inhibitor NVP-BEZ235 against T-cell acute lymphoblastic leukemia. *Cancer Res.* 70:8097–8107. http://dx.doi.org/10.1158/0008-5472.CAN-10-1814

Chan, S.M., A.P. Weng, R. Tibshirani, J.C. Aster, and P.J. Utz. 2007. Notch signals positively regulate activity of the mTOR pathway in T-cell acute lymphoblastic leukemia. *Blood*. 110:278–286. http://dx.doi.org/10.1182/blood-2006-08-039883

Cho, S.H., S. Goenka, T. Henttinen, P. Gudapati, A. Reinikainen, C.M. Eischen, R. Lahesmaa, and M. Boothby. 2009. PARP-14, a member of the B aggressive lymphoma family, transduces survival signals in primary B cells. *Blood*. 113:2416–2425. http://dx.doi.org/10.1182/blood-2008-03-144121

Ciofani, M., and J.C. Zúñiga-Pflücker. 2005. Notch promotes survival of pre-T cells at the β-selection checkpoint by regulating cellular metabolism. *Nat. Immunol.* 6:881–888. http://dx.doi.org/10.1038/ni1234

Collins, B.J., M. Deak, J.S. Arthur, L.J. Armit, and D.R. Alessi. 2003. In vivo role of the PIF-binding docking site of PDK1 defined by knock-in mutation. *EMBO J.* 22:4202–4211. http://dx.doi.org/10.1093/emboj/cdg407

Cully, M., H. You, A.J. Levine, and T.W. Mak. 2006. Beyond PTEN mutations: the PI3K pathway as an integrator of multiple inputs during tumorigenesis. *Nat. Rev. Cancer*. 6:184–192. http://dx.doi.org/10.1038/nrc1819

Dan, H.C., M.J. Cooper, P.C. Cogswell, J.A. Duncan, J.P. Ting, and A.S. Baldwin. 2008. Akt-dependent regulation of NF-κB is controlled by mTOR and Raptor in association with IKK. *Genes Dev.* 22:1490–1500. http://dx.doi.org/10.1101/gad.1662308

de Boer, J., A. Williams, G. Skavdis, N. Harker, M. Coles, M. Tolaini, T. Norton, K. Williams, K. Roderick, A.J. Potocnik, and D. Kioussis. 2003. Transgenic mice with hematopoietic and lymphoid specific expression of Cre. *Eur. J. Immunol.* 33:314–325. http://dx.doi.org/10.1002/immu.200310005

Delgoffe, G.M., K.N. Pollizzi, A.T. Waickman, E. Heikamp, D.J. Meyers, M.R. Horton, B. Xiao, P.F. Worley, and J.D. Powell. 2011. The kinase mTOR regulates the differentiation of helper T cells through the selective activation of signaling by mTORC1 and mTORC2. *Nat. Immunol.* 12:295–303. http://dx.doi.org/10.1038/ni.2005

Eng, C. 2003. PTEN: one gene, many syndromes. *Hum. Mutat.* 22:183–198. http://dx.doi.org/10.1002/humu.10257

Espinosa, L., S. Cathelin, T. D'Altri, T. Trimarchi, A. Statnikov, J. Guiu, V. Rodilla, J. Inglés-Esteve, J. Nomdedeu, B. Bellosillo, et al. 2010. The Notch/Hes1 pathway sustains NF-κB activation through CYLD repression in T cell leukemia. *Cancer Cell*. 18:268–281. http://dx.doi.org/10.1016/j.ccr.2010.08.006

Facchinetti, V., W. Ouyang, H. Wei, N. Soto, A. Lazorchak, C. Gould, C. Lowry, A.C. Newton, Y. Mao, R.Q. Miao, et al. 2008. The mammalian target of rapamycin complex 2 controls folding and stability of Akt and protein kinase C. *EMBO J.* 27:1932–1943. http://dx.doi.org/10.1038/emboj.2008.120

Feng, J., J. Park, P. Cron, D. Hess, and B.A. Hemmings. 2004. Identification of a PKB/Akt hydrophobic motif Ser-473 kinase as DNA-dependent protein kinase. *J. Biol. Chem.* 279:41189–41196. http://dx.doi.org/10.1074/jbc.M406731200

García-Martínez, J.M., and D.R. Alessi. 2008. mTOR complex 2 (mTORC2) controls hydrophobic motif phosphorylation and activation of serum- and glucocorticoid-induced protein kinase 1 (SGK1). *Biochem. J.* 416:375–385. http://dx.doi.org/10.1042/BJ20081668

Guertin, D.A., and D.M. Sabatini. 2009. The pharmacology of mTOR inhibition. *Sci. Signal.* 2:pe24. http://dx.doi.org/10.1126/scisignal.267pe24

Guertin, D.A., D.M. Stevens, C.C. Thoreen, A.A. Burds, N.Y. Kalaany, J. Moffat, M. Brown, K.J. Fitzgerald, and D.M. Sabatini. 2006. Ablation in mice of the mTORC components raptor, rictor, or mLST8 reveals that mTORC2 is required for signaling to Akt-FOXO and PKCalpha, but not S6K1. *Dev. Cell*. 11:859–871. http://dx.doi.org/10.1016/j.devcel.2006.10.007

Gutierrez, A., T. Sanda, R. Grebliunaite, A. Carracedo, L. Salmena, Y. Ahn, S. Dahlberg, D. Neuberg, L.A. Moreau, S.S. Winter, et al. 2009. High frequency of PTEN, PI3K, and AKT abnormalities in T-cell acute lymphoblastic leukemia. *Blood*. 114:647–650. http://dx.doi.org/10.1182/blood-2009-02-206722

Harada, Y., Y. Harada, C. Elly, G. Ying, J.H. Paik, R.A. DePinho, and Y.C. Liu. 2010. Transcription factors Foxo3a and Foxo1 couple the E3 ligase Cbl-b to the induction of Foxp3 expression in induced regulatory T cells. *J. Exp. Med.* 207:1381–1391. http://dx.doi.org/10.1084/jem.20100004

Hasegawa, H., T. Nomura, M. Kohno, N. Tateishi, Y. Suzuki, N. Maeda, R. Fujisawa, O. Yoshie, and S. Fujita. 2000. Increased chemokine receptor CCR7/EBI1 expression enhances the infiltration of lymphoid organs by adult T-cell leukemia cells. *Blood*. 95:30–38.

Hayday, A.C., and D.J. Pennington. 2007. Key factors in the organized chaos of early T cell development. *Nat. Immunol.* 8:137–144. http://dx.doi.org/10.1038/ni1436

Hinton, H.J., D.R. Alessi, and D.A. Cantrell. 2004. The serine kinase phosphoinositide-dependent kinase 1 (PDK1) regulates T cell development. *Nat. Immunol.* 5:539–545. http://dx.doi.org/10.1038/ni1062

Ikenoue, T., K. Inoki, Q. Yang, X. Zhou, and K.L. Guan. 2008. Essential function of TORC2 in PKC and Akt turn motif phosphorylation, maturation and signalling. *EMBO J.* 27:1919–1931. http://dx.doi.org/10.1038/emboj.2008.119

Jacinto, E., V. Facchinetti, D. Liu, N. Soto, S. Wei, S.Y. Jung, Q. Huang, J. Qin, and B. Su. 2006. SIN1/MIP1 maintains rictor-mTOR complex integrity and regulates Akt phosphorylation and substrate specificity. *Cell*. 127:125–137. http://dx.doi.org/10.1016/j.cell.2006.08.033

Janes, M.R., J.J. Limon, L. So, J. Chen, R.J. Lim, M.A. Chavez, C. Vu, M.B. Lilly, S. Mallya, S.T. Ong, et al. 2010. Effective and selective targeting of leukemia cells using a TORC1/2 kinase inhibitor. *Nat. Med.* 16:205–213. http://dx.doi.org/10.1038/nm.2091

Jones, R.G., S.D. Saibil, J.M. Pun, A.R. Elford, M. Bonnard, M. Pellegrini, S. Arya, M.E. Parsons, C.M. Krawczyk, S. Gerondakis, et al. 2005. NF-kappaB couples protein kinase B/Akt signaling to distinct survival pathways and the regulation of lymphocyte homeostasis in vivo. *J. Immunol.* 175:3790–3799.

Jongen-Lavrencic, M., S. Salesse, R. Delwel, and C.M. Verfaillie. 2005. BCR/ABL-mediated downregulation of genes implicated in cell adhesion and motility leads to impaired migration toward CCR7 ligands CCL19 and CCL21 in primary BCR/ABL-positive cells. *Leukemia*. 19:373–380. http://dx.doi.org/10.1038/sj.leu.2403626

Juntilla, M.M., J.A. Wofford, M.J. Birnbaum, J.C. Rathmell, and G.A. Koretzky. 2007. Akt1 and Akt2 are required for alphabeta thymocyte survival and differentiation. *Proc. Natl. Acad. Sci. USA*. 104:12105–12110. http://dx.doi.org/10.1073/pnas.0705285104

Kawakami, Y., H. Nishimoto, J. Kitaura, M. Maeda-Yamamoto, R.M. Kato, D.R. Littman, M. Leitges, D.J. Rawlings, and T. Kawakami. 2004. Protein kinase C betaII regulates Akt phosphorylation on Ser-473 in a cell type- and stimulus-specific fashion. *J. Biol. Chem.* 279:47720–47725. http://dx.doi.org/10.1074/jbc.M408797200

Kelly, A.P., D.K. Finlay, H.J. Hinton, R.G. Clarke, E. Fiorini, F. Radtke, and D.A. Cantrell. 2007. Notch-induced T cell development requires phosphoinositide-dependent kinase 1. *EMBO J.* 26:3441–3450. http://dx.doi.org/10.1038/sj.emboj.7601761

Laplante, M., and D.M. Sabatini. 2009. mTOR signaling at a glance. *J. Cell Sci.* 122:3589–3594. http://dx.doi.org/10.1242/jcs.051011

Lee, K.Y., F. D'Acquisto, M.S. Hayden, J.H. Shim, and S. Ghosh. 2005. PDK1 nucleates T cell receptor-induced signaling complex for NF-kappaB activation. *Science*. 308:114–118. http://dx.doi.org/10.1126/science.1107107

Lee, K.W., Y. Lee, D.S. Kim, and H.J. Kwon. 2006. Direct role of NF-kappaB activation in Toll-like receptor-triggered HLA-DRA expression. *Eur. J. Immunol.* 36:1254–1266. http://dx.doi.org/10.1002/eji.200535577

Lee, K., P. Gudapati, S. Dragovic, C. Spencer, S. Joyce, N. Killeen, M.A. Magnuson, and M. Boothby. 2010. Mammalian target of rapamycin protein complex 2 regulates differentiation of Th1 and Th2 cell subsets via distinct signaling pathways. *Immunity*. 32:743–753. http://dx.doi.org/10.1016/j.immuni.2010.06.002

Li, J., C. Yen, D. Liaw, K. Podsypanina, S. Bose, S.I. Wang, J. Puc, C. Miliaresis, L. Rodgers, R. McCombie, et al. 1997. PTEN, a putative protein tyrosine phosphatase gene mutated in human brain, breast, and prostate cancer. *Science*. 275:1943–1947. http://dx.doi.org/10.1126/science.275.5308.1943

Luo, H., W. Duguid, H. Chen, M. Maheu, and J. Wu. 1994. The effect of rapamycin on T cell development in mice. *Eur. J. Immunol.* 24:692–701. http://dx.doi.org/10.1002/eji.1830240331

Maillard, I., T. Fang, and W.S. Pear. 2005. Regulation of lymphoid development, differentiation, and function by the Notch pathway. *Annu. Rev. Immunol.* 23:945–974. http://dx.doi.org/10.1146/annurev.immunol.23.021704.115747

Mao, C., E.G. Tili, M. Dose, M.C. Haks, S.E. Bear, I. Maroulakou, K. Horie, G.A. Gaitanaris, V. Fidanza, T. Ludwig, et al. 2007. Unequal

contribution of Akt isoforms in the double-negative to double-positive thymocyte transition. *J. Immunol.* 178:5443–5453.

Maser, R.S., B. Choudhury, P.J. Campbell, B. Feng, K.K. Wong, A. Protopopov, J. O'Neil, A. Gutierrez, E. Ivanova, I. Perna, et al. 2007. Chromosomally unstable mouse tumours have genomic alterations similar to diverse human cancers. *Nature.* 447:966–971. http://dx.doi.org/10.1038/nature05886

Medyouf, H., X. Gao, F. Armstrong, S. Gusscott, Q. Liu, A.L. Gedman, L.H. Matherly, K.R. Schultz, F. Pflumio, M.J. You, and A.P. Weng. 2010. Acute T-cell leukemias remain dependent on Notch signaling despite PTEN and INK4A/ARF loss. *Blood.* 115:1175–1184. http://dx.doi.org/10.1182/blood-2009-04-214718

Nakamura, N., S. Ramaswamy, F. Vazquez, S. Signoretti, M. Loda, and W.R. Sellers. 2000. Forkhead transcription factors are critical effectors of cell death and cell cycle arrest downstream of PTEN. *Mol. Cell. Biol.* 20: 8969–8982. http://dx.doi.org/10.1128/MCB.20.23.8969-8982.2000

O'Neil, J., J. Calvo, K. McKenna, V. Krishnamoorthy, J.C. Aster, C.H. Bassing, F.W. Alt, M. Kelliher, and A.T. Look. 2006. Activating Notch1 mutations in mouse models of T-ALL. *Blood.* 107:781–785. http://dx.doi.org/10.1182/blood-2005-06-2553

Ouyang, W., O. Beckett, Q. Ma, J.H. Paik, R.A. DePinho, and M.O. Li. 2010. Foxo proteins cooperatively control the differentiation of Foxp3$^+$ regulatory T cells. *Nat. Immunol.* 11:618–627. http://dx.doi.org/10.1038/ni.1884

Ozes, O.N., L.D. Mayo, J.A. Gustin, S.R. Pfeffer, L.M. Pfeffer, and D.B. Donner. 1999. NF-kappaB activation by tumour necrosis factor requires the Akt serine-threonine kinase. *Nature.* 401:82–85. http://dx.doi.org/10.1038/43466

Radtke, F., A. Wilson, G. Stark, M. Bauer, J. van Meerwijk, H.R. MacDonald, and M. Aguet. 1999. Deficient T cell fate specification in mice with an induced inactivation of Notch1. *Immunity.* 10:547–558. http://dx.doi.org/10.1016/S1074-7613(00)80054-0

Ranganathan, P., K.L. Weaver, and A.J. Capobianco. 2011. Notch signalling in solid tumours: a little bit of everything but not all the time. *Nat. Rev. Cancer.* 11:338–351. http://dx.doi.org/10.1038/nrc3035

Real, P.J., and A.A. Ferrando. 2009. NOTCH inhibition and glucocorticoid therapy in T-cell acute lymphoblastic leukemia. *Leukemia.* 23:1374–1377. http://dx.doi.org/10.1038/leu.2009.75

Real, P.J., V. Tosello, T. Palomero, M. Castillo, E. Hernando, E. de Stanchina, M.L. Sulis, K. Barnes, C. Sawai, I. Homminga, et al. 2009. Gamma-secretase inhibitors reverse glucocorticoid resistance in T cell acute lymphoblastic leukemia. *Nat. Med.* 15:50–58. http://dx.doi.org/10.1038/nm.1900

Romashkova, J.A., and S.S. Makarov. 1999. NF-kappaB is a target of AKT in anti-apoptotic PDGF signalling. *Nature.* 401:86–90. http://dx.doi.org/10.1038/43474

Sarbassov, D.D., S.M. Ali, D.H. Kim, D.A. Guertin, R.R. Latek, H. Erdjument-Bromage, P. Tempst, and D.M. Sabatini. 2004. Rictor, a novel binding partner of mTOR, defines a rapamycin-insensitive and raptor-independent pathway that regulates the cytoskeleton. *Curr. Biol.* 14:1296–1302. http://dx.doi.org/10.1016/j.cub.2004.06.054

Sarbassov, D.D., D.A. Guertin, S.M. Ali, and D.M. Sabatini. 2005. Phosphorylation and regulation of Akt/PKB by the rictor-mTOR complex. *Science.* 307:1098–1101. http://dx.doi.org/10.1126/science.1106148

Sarbassov, D.D., S.M. Ali, S. Sengupta, J.H. Sheen, P.P. Hsu, A.F. Bagley, A.L. Markhard, and D.M. Sabatini. 2006. Prolonged rapamycin treatment inhibits mTORC2 assembly and Akt/PKB. *Mol. Cell.* 22:159–168. http://dx.doi.org/10.1016/j.molcel.2006.03.029

Schmitt, T.M., M. Ciofani, H.T. Petrie, and J.C. Zúñiga-Pflücker. 2004. Maintenance of T cell specification and differentiation requires recurrent notch receptor-ligand interactions. *J. Exp. Med.* 200:469–479. http://dx.doi.org/10.1084/jem.20040394

Searfoss, G.H., W.H. Jordan, D.O. Calligaro, E.J. Galbreath, L.M. Schirtzinger, B.R. Berridge, H. Gao, M.A. Higgins, P.C. May, and T.P. Ryan. 2003. Adipsin, a biomarker of gastrointestinal toxicity mediated by a functional gamma-secretase inhibitor. *J. Biol. Chem.* 278:46107–46116. http://dx.doi.org/10.1074/jbc.M307757200

Shiota, C., J.T. Woo, J. Lindner, K.D. Shelton, and M.A. Magnuson. 2006. Multiallelic disruption of the rictor gene in mice reveals that mTOR complex 2 is essential for fetal growth and viability. *Dev. Cell.* 11:583–589. http://dx.doi.org/10.1016/j.devcel.2006.08.013

Tandon, P., C.A. Gallo, S. Khatri, J.F. Barger, H. Yepiskoposyan, and D.R. Plas. 2011. Requirement for ribosomal protein S6 kinase 1 to mediate glycolysis and apoptosis resistance induced by Pten deficiency. *Proc. Natl. Acad. Sci. USA.* 108:2361–2365. http://dx.doi.org/10.1073/pnas.1013629108

Tanigaki, K., M. Tsuji, N. Yamamoto, H. Han, J. Tsukada, H. Inoue, M. Kubo, and T. Honjo. 2004. Regulation of alphabeta/gammadelta T cell lineage commitment and peripheral T cell responses by Notch/RBP-J signaling. *Immunity.* 20:611–622. http://dx.doi.org/10.1016/S1074-7613(04)00109-8

Vacca, A., M.P. Felli, R. Palermo, G. Di Mario, A. Calce, M. Di Giovine, L. Frati, A. Gulino, and I. Screpanti. 2006. Notch3 and pre-TCR interaction unveils distinct NF-kappaB pathways in T-cell development and leukemia. *EMBO J.* 25:1000–1008. http://dx.doi.org/10.1038/sj.emboj.7600996

Vanhaesebroeck, B., and D.R. Alessi. 2000. The PI3K-PDK1 connection: more than just a road to PKB. *Biochem. J.* 346:561–576. http://dx.doi.org/10.1042/0264-6021:3460561

Vilimas, T., J. Mascarenhas, T. Palomero, M. Mandal, S. Buonamici, F. Meng, B. Thompson, C. Spaulding, S. Macaroun, M.L. Alegre, et al. 2007. Targeting the NF-kappaB signaling pathway in Notch1-induced T-cell leukemia. *Nat. Med.* 13:70–77. http://dx.doi.org/10.1038/nm1524

Volanakis, E.J., R.T. Williams, and C.J. Sherr. 2009. Stage-specific Arf tumor suppression in Notch1-induced T-cell acute lymphoblastic leukemia. *Blood.* 114:4451–4459. http://dx.doi.org/10.1182/blood-2009-07-233346

Voll, R.E., E. Jimi, R.J. Phillips, D.F. Barber, M. Rincon, A.C. Hayday, R.A. Flavell, and S. Ghosh. 2000. NF-κ B activation by the pre-T cell receptor serves as a selective survival signal in T lymphocyte development. *Immunity.* 13:677–689. http://dx.doi.org/10.1016/S1074-7613(00)00067-4

Waugh, C., L. Sinclair, D. Finlay, J.R. Bayascas, and D. Cantrell. 2009. Phosphoinositide (3,4,5)-triphosphate binding to phosphoinositide-dependent kinase 1 regulates a protein kinase B/Akt signaling threshold that dictates T-cell migration, not proliferation. *Mol. Cell. Biol.* 29:5952–5962. http://dx.doi.org/10.1128/MCB.00585-09

Weng, A.P., A.A. Ferrando, W. Lee, J.P. Morris IV, L.B. Silverman, C. Sanchez-Irizarry, S.C. Blacklow, A.T. Look, and J.C. Aster. 2004. Activating mutations of NOTCH1 in human T cell acute lymphoblastic leukemia. *Science.* 306:269–271. http://dx.doi.org/10.1126/science.1102160

Xie, X., D. Zhang, B. Zhao, M.K. Lu, M. You, G. Condorelli, C.Y. Wang, and K.L. Guan. 2011. IkappaB kinase ε and TANK-binding kinase 1 activate AKT by direct phosphorylation. *Proc. Natl. Acad. Sci. USA.* 108:6474–6479. http://dx.doi.org/10.1073/pnas.1016132108